January 1994

The Source Hydrology of Severe Sustained Drought in th Southwestern U.S.

David G. Tarboton

published in the Journal of Hydrology. 161: 31-69, 1994

The Source Hydrology of Severe Sustained Drought in the Southwestern U.S.

David G Tarboton

Executive Summary

Highly developed water storage and distribution systems in the southwestern United States provide security against local droughts of short duration. However these large interlinked storage and distribution systems are now susceptible to sustained regional shortages of water supply. This paper develops hydrologic scenarios of regional shortage to be used in the broader study of the economic, political, social and environmental impacts of severe sustained drought in the southwestern U.S. This paper has developed severe sustained drought scenarios for the Colorado River and four major rivers of northern California based on recorded streamflow as well as streamflow reconstructions from tree ring measurements. These are sustained droughts identified from consideration of storage deficit criteria and will be critical in well developed water supply systems with large storage. They do not necessarily include some severe short droughts.

The scenarios are:

1. Colorado River Basin Severe Drought. The period 1579 to 1600 is the most severe sustained drought that occurred in the tree ring reconstruction of Lees Ferry streamflow (Stockton and Jacoby, 1976) dating back to 1520. It is characterized by a 22 year mean streamflow of 11.1 MAF[1] with mean streamflow over the first 17 years (1579 to 1595) of only 10.5 MAF. The mean of recorded streamflow at Lees Ferry is 15.2 MAF. This drought is estimated to have a return period between 400 to 700 years.

2. California Severe Drought. The period 1918 to 1939 is the most severe sustained drought that occurred in the recorded natural streamflow in the California four rivers index (Sacramento, American, Yuba and Feather river flows combined) dating to 1906. It is characterized by a 21 year mean flow of 13.7 MAF, compared the mean of recorded streamflow of 17.8 MAF. The return period is estimated to be between 80 and 180 years. This was more severe than any droughts in a tree ring reconstruction of the four rivers index (Earle and Fritts, 1986) dating back to 1560. However this particular tree ring reconstruction is not well correlated (cross correlation = 0.45) with observed streamflow.

---

[1] The units used for streamflow are million acre-feet (MAF) per year. (= 1.23×10^9 m^3)

3. Colorado Drought in Historic Record. The period 1943 to 1964 is the most severe drought that occurred in the observed Lees Ferry streamflow record dating to 1906. It is characterized by a 22 year mean flow of 13.4 MAF (observed mean 15.2 MAF). The return period is estimated to be between 50 and 100 years. This drought is defensible as likely to recur regardless of uncertainty in the tree ring reconstructions of streamflow.

4. Colorado Rearranged Severe Drought. This is an artificial scenario formed by taking the flows in scenario 1 above and assuming they occur in decreasing order so that the lowest flows come at the end. It is characterized by a 16 year mean flow of 9.6 MAF (observed mean 15.2 MAF) and has return period from 2000 to 10,000 years or more. This is an extreme, perhaps even unrealistic scenario, designed to discover how the system would respond to a truly catastrophic drought.

Because drought is by definition a rare event the number of occurrences in the observed streamflow record, of length about 80 years, is small, so the risk assessments are uncertain. Tree ring reconstructions of streamflow offer a physical basis for the extension of hydrologic records further back than observed records and thus provide a window into the past that yields additional information on the magnitude and frequency of droughts. Tree ring streamflow reconstructions are however far from perfect and their limitations need to be recognized. Two independent tree ring reconstructions of streamflow at Lees Ferry were available (Stockton and Jacoby, 1976; Michaelson et al., 1990) and although both had respectable and comparable cross correlations with observed flow (0.76 and 0.77) significant differences were noted. The estimates of drought risk, reported above in terms of return period, associated with the drought scenarios developed, attempt to account for this uncertainty and were developed considering the length of record available and results from a range of plausable stochastic models for annual streamflow. These included independent, autoregressive order one, and fractional Gaussian noise models. The risk of joint occurrence of sustained drought in the Colorado River and California was also calculated and found to occur nearly as frequently as drought in either region considered separately. These occurrence risks should be borne in mind when evaluating and developing planning strategies based on these scenarios.

Since scenarios 1 and 4 were defined in terms of Lees Ferry tree ring reconstructed streamflow to use them with the Colorado River System Simulation model required disaggregation into the source inflow at each of 29 source flow locations. This was done using a statistical disaggregation package (Grygier and Stedinger, 1988). Because of the size of this disaggregation problem visual graphical techniques, such as the boxplot and non parametric density estimate, were

extensively used to validate the disaggregation model.

References

Earle, C. J. and H. C. Fritts, 1986. Reconstructing Riverflow in the Sacramento Basin Since 1560. Report to California Department of Water Resources, Agreement No. DWR B-55398. Laboratory of Tree Ring Research, University of Arizona, Tuscon.

Grygier, J. C. and J. R. Stedinger, 1988. Condensed Disaggregation Procedures and Conservation Corrections for Stochastic Hydrology. Water Resources Research, 24(10): 1574-1584.

Michaelson, J., H. A. Loaiciga, L. Haston and S. Garver, 1990. Estimating drought probabilities in California using tree rings. Completion report to California Department of Water Resources, Department of Geography, University of California, Santa Barbara.

Stockton, C. W. and G. C. Jacoby, 1976. Long-Term Surface-Water Supply and Streamflow Trends in the Upper Colorado River Basin Based on Tree-Ring Analyses. Lake Powell Research Project Bulletin, No. 18, National Science Foundation.

The Source Hydrology of Severe Sustained Drought in the Southwestern United States

David G Tarboton
Utah Water Research Laboratory
Utah State University
Logan, UT, 84322-8200

Revised and submitted to Journal of Hydrology, March 1994.

Abstract

This paper considers the risk of drought and develops drought scenarios for use in the study of severe sustained drought in the Southwestern United States. The focus is on the Colorado River basin and regions to which Colorado River water is exported, especially southern California, which depends on water from the Colorado River as well as the four major rivers in northern California. Drought scenarios are developed using estimates of unimpaired historic streamflow as well as reconstructions of streamflow based on tree ring widths. Drought scenarios in the Colorado River are defined on the basis of annual flow at Lees Ferry. Possible spatial manifestations of the Colorado River drought scenarios for input into a Colorado River system simulation model are developed by disaggregating the Lees Ferry flow to monthly flows at twenty nine source locations required by the model. The risk, in terms of return period, of the drought scenarios developed, is assessed using stochastic models applied to both the Colorado River basin and the combined flow in four major California rivers. The risks of severe sustained drought occurring concurrently in the Colorado River basin and California is also assessed.

Introduction

The inherent scarcity of water in the semi-arid to arid regions of the southwestern United States (Figure 1) is exacerbated by the occurrence of frequent and persistent droughts (Stockton et al., 1991). The impact of these droughts is constantly changing as the growing population places increased demands on supplies. This is countered by the development of storage and distribution systems that can store water for up to decades and transport water thousands of miles. These measures provide security against local shortages of short duration but effectively interlink large regions. However these large interlinked storage and distribution systems are now susceptible to sustained regional shortages of water supply.

This paper describes the hydrology work done as part of a multidisciplinary study to assess the likely impact of and to develop a contingency plan for severe sustained drought in the region served by the Colorado River. This includes the Colorado River basin as well as areas that have grown to depend on Colorado River water, such as southern California and parts of Colorado, Utah, Arizona and New Mexico that are technically not within the Colorado River basin. Figure 1 is a schematic of the study area. Most of the streamflow in the Colorado River comes from snowmelt in the Rocky mountains in Colorado, Utah and Wyoming. Several reservoirs, the largest of which are Lake Powell and Lake Mead provide storage, hydro electric power and flood control. The use of water from the Colorado River is strictly controlled and governed by a complex system of law centered on the Colorado River compact. This apportions water between the upper and lower divisions of the Colorado River basin. Water is apportioned among states by other compacts and court decrees. Some of the water supply systems for utilization of this water are indicated in Figure 1. Southern California and in particular the metropolitan area surrounding Los Angeles draws water from the Colorado River, via the Colorado River aqueduct and from northern California via a series of canals pumping from the Sacramento river delta that comprise the state water project. Four major rivers in northern California, the Sacramento River, Yuba River, American River and Feather River combine to provide water into the Sacramento River delta. For drought impacts on southern California the possibility of simultaneous shortage in the Colorado River and the four northern California rivers are considered.

In this paper critical periods of shortage in the historic and paleo (tree ring) streamflow record are identified. These are used to develop study scenarios. They are also used to characterize the spatial distribution of supply during these scenarios and to assess the risk or

likelihood of occurrence of these scenarios.

The sources of data upon which this work was based consisted of the following unimpaired streamflow estimates and streamflow reconstructed from the measurement of tree ring widths.

1. Historic unimpaired streamflow at 29 sites in the Colorado River basin, 1906-1983 (78 years) as estimated by the U.S. Bureau of Reclamation.
2. Combined total historic unimpaired streamflow in the Sacramento, Yuba, Feather and American rivers in California, 1906-1991 (86 years) as estimated by the California Department of Water Resources. This is called the California four rivers index.
3. Tree ring reconstructed streamflow at Lees Ferry on the Colorado River, 1520-1961 (442 years) from Stockton and Jacoby (1976).
4. Tree ring reconstructed streamflow at Lees Ferry on the Colorado River, 1568-1962 (395 years) from Michaelson et al. (1990).
5. Tree ring reconstructed California four rivers index streamflow, 1560-1980 (421 years) from Earle and Fritts (1986).

Streamflow at Lees Ferry is used in this paper to refer to streamflow at the Colorado River compact point near Lees Ferry, Arizona, defined as a point one mile downstream of the confluence of the Colorado and Paria rivers. This is the sum of streamflow measured at the Lees Ferry gage upstream of the Paria confluence and Paria gage. The compact point legally subdivides the Colorado River basin into upper and lower divisions.

Unimpaired streamflow is measured streamflow adjusted for anthropogenic consumptive use and reservoir operations. It is an estimate of what streamflow would have been had the basins remained in their natural state.

Tree ring studies offer a physical basis for the extension of hydrologic records further back than observed records, and thus provide a window into the past that may yield additional information on the possible magnitude and frequency of the occurrence of droughts. These record extensions do not suffer from the uncertainty associated with stochastically generated sequences, but do contain uncertainty associated with the relationship between tree ring widths and streamflows. Despite these drawbacks, tree rings often provide the only physically realistic glimpse of past hydrologic conditions which could recur and should be planned for. The approach in this work was to take advantage of the information provided by tree ring reconstructions of streamflow to identify and develop severe drought scenarios. To allay scepticism regarding the use

of tree ring reconstructed streamflow one drought scenario based only on recorded streamflow was used.

Stochastic techniques were used to disaggregate basin total annual streamflows reconstructed from tree rings into monthly flows at the individual control points used by the system simulation model. Stochastic techniques were also used to assess the risk of the scenarios developed from tree ring studies.

The primary product from this work was drought scenarios disaggregated spatially into monthly flows at each of the Colorado River source locations shown in Figure 1. These results were intended for use by other investigators in simulation and impact analysis models such as the Colorado River Model (Brown et al., 1990; Brown et al., 1988). This model which emulates and extends the U.S. Bureau of Reclamation's Colorado River Simulation Model is distributed by Hydrosphere, Boulder, Colorado and includes as an input option the inflow scenarios developed here.

The first section below expands on the approach and the rationale for the use of a combination of stochastic hydrologic techniques and tree ring reconstructions. The next section describes the identification and selection of the drought scenarios used in this work. A section addressing the spatial variability of supply and the procedures used to disaggregate regional flows spatially into the flows required for simulation of the operation of the Colorado River reservoir and distribution systems follows. The last section addresses the risk, or likelihood of occurrence of the study scenarios used. This assessment is necessarily imprecise because it is based on a limited number of occurrences of severe sustained drought in the historical and tree ring reconstructed record.

Stochastic Hydrology and Tree Ring Reconstructions

The goal of stochastic hydrology for many years has been to generate synthetic streamflow sequences statistically equivalent to observed streamflow sequences to test water resource systems. Following the first early studies (Thomas and Fiering, 1962; Fiering, 1967) the technique has developed considerably and is described in many journal articles and text books (Maidment, 1993; Bras and Rodriguez-Iturbe, 1985; Salas et al., 1980; Yevjevich, 1972). However, despite considerable success, stochastic hydrology has its limitations. The observed streamflow record is of limited length. If the goal is to study rare drought events the recorded flow will not contain

many of these, so the sample size is small. Models used to simulate streamflow sequences are almost always stationary. Yet stationarity can seldom be proved for streamflows and arguments for persistence due to non-stationarity and the impropriety of using stationary short memory processes to simulate streamflow have been advanced (Wallis, 1977). There is always considerable uncertainty in the parameters of models used to characterize and generate synthetic streamflows, and these uncertainties may have considerable impact on resultant required storage and yield in water supply systems (Rodr'guez-Iturbe, 1969; Stedinger et al., 1985). This uncertainty can be accounted for by treating the parameters as random variables and generating them stochastically from estimates of their sampling distributions (Stedinger et al., 1985; Grygier and Stedinger, 1990a; Grygier and Stedinger, 1988). While it is important to acknowledge uncertainty in model parameters, simulations based on uncertain parameters can sometimes lead to streamflows that are not credible to practicing water managers and their agencies.

These problems and limitations with stochastic simulation have led to scepticism in some water agencies that try to use these techniques. An alternative empirical procedure, the index sequential method, appears to be the method of choice in many agencies (Kendall and Dracup, 1991a; 1991b). The index sequential method uses only the historic flow sequence and synthesizes the same number of sequences as there are years in the historic record. Each sequence differs from the next only by the fact that the first streamflow year is incremented by one and the first year is transferred to the end of the sequence. Drawbacks of testing designs against only the historical flows have been emphasized (Loucks et al., 1981), particularly for systems with large amounts of over-year storage, such as the Colorado River basin.

The use of tree ring width measurements to reconstruct past hydrology (dendrohydrology) has been well documented (Loaiciga et al., 1993; Cook and Kairiukstis, 1990; Fritts, 1976; Stockton and Jacoby, 1976; Stockton and Boggess, 1979; Stockton et al., 1991; Michaelson et al., 1990). These reconstructions are not without problems. Tree ring widths are related to moisture availability at the site in which the trees are growing and are not spatially integrated measures of conditions over a whole river basin. Tree ring widths are more sensitive to lack of precipitation, which limits growth than they are to abundant precipitation during which time other factors than water may limit growth. This may impose a bias towards sensitivity to dry conditions in tree ring data. Precipitation that does not impact tree growth, for whatever reason, will not be reflected in the tree ring record. This may include precipitation not on sampled forested areas, or that does not infiltrate, or that occurs outside the growing season.

Also raw tree ring widths are non-stationary, due to biological age related growth trends. This non-stationarity is removed from the raw ring width data using empirical detrending techniques to get stationary growth indices that are then correlated with streamflow (Stockton and Jacoby, 1976; Loaiciga et al., 1993). This may have the effect of removing any non-stationarity in the precipitation and moisture availability that would have been present in past streamflows.

Figures 2, 3, and 4 compare observed and tree ring reconstructions of streamflow in the Colorado River at Lees Ferry and California four river index. The Colorado River streamflow reconstructions are regarded in the tree ring literature as adequate (Michaelson et al., 1990; Stockton and Jacoby, 1976). The cross correlation between observed and reconstructed streamflow is 0.76 for the Stockton and Jacoby reconstruction and 0.77 for the Michaelson et al. reconstruction. The California four river index reconstruction is on the other hand less satisfactory (Stockton et al., 1991) with cross correlation between observed and reconstructed streamflow of 0.45. Table 1 gives statistics of the observed and reconstructed streamflow series. Notice that since the reconstructed streamflow is obtained from regression of tree ring width indices against the observed streamflow, the unexplained variance is omitted, resulting in smaller standard deviations in the reconstructed, as compared to observed streamflow.

One feature of the Lees Ferry reconstruction is an apparent difference in the mean over the period of recorded flows (15.2 million acre-feet[1], MAF) from that of the reconstructed flows (13.5 MAF) (see Figure 3). A t test indicates that this difference is significant ($t > 3$, $\alpha < 0.004$). This is also strikingly evident in Figure 5 where the cumulative departures from the tree ring reconstructed mean show a steady increase during the period of recorded flow but a less steady decrease during the period of reconstruction. This apparent non-stationarity is of concern because any non-stationarity was intended to have been removed from tree ring indices before correlation with streamflow. This feature is apparent in both Lees Ferry reconstructions.

The differences between the two Colorado reconstructions are disturbing and could have a significant impact on planning strategies. The 10 year moving averages (Figure 4) sometimes differ by as much as 2 MAF between the two reconstructions when compared to a mean of 13.5 MAF. This occurs immediately after a sustained severe drought from 1600 to 1630 and could be important for recovery of the system. It also occurs from 1800 to 1830 where one reconstruction

[1] The units used for streamflow are either million acre-feet (MAF) per year or thousand acre-feet (KAF) per year. 1 acre-foot is 1.23×10^3 m^3.

is in a drought and the other in surplus. However differences such as these are reportedly typical statistical discrepancies in these type of tree ring studies (Loaiciga et al., 1992; 1993).

These uncertainties are manifested in the sometimes poor correlation between tree ring reconstructions and observed flows, this over the period of calibration. It is probably safe to assume that this correlation will be worse over the period of reconstruction.

The Michaelson et al. (1990) reconstruction is based on five tree ring chronologies, chosen from a set of 29 chronologies considered. Growth curves were removed using robust local regression (lowess), and auto regressive models were used to pre-whiten the tree ring indices. Mallows Cp criterion was used in the multiple linear regression to select the five chronologies "that combined as the most precise retrodictor of flow in the area". The Stockton and Jacoby (1976) reconstruction is actually the average of two reconstructions using a total of 18 tree ring chronologies. Least squares fitting of a modified exponential form is used to remove growth curves and multiple linear regression against significant eigenvectors (principal components) of the tree ring data grid is used for the reconstruction. Since the cross correlation between observed and predicted streamflow is essentially equivalent for these reconstructions (0.76 versus 0.77) we prefer the Stockton and Jacoby reconstruction since it is based on a greater spatial distribution of trees and is therefore less likely to suffer from the problems listed above, namely flow generated from areas where tree rings were not sampled. The remainder of this work is therefore based on the Stockton and Jacoby (1976) reconstruction.

Identification of Droughts and Drought Scenarios

Several options are available for the identification of severe sustained droughts in a flow record. Some of these are:

a) The drought with the maximum deficit magnitude (largest accumulated deficit below the mean annual flow over a continuous period with flow below the mean).

b) The drought that would cause the greatest reservoir depletion in a storage deficit analysis with fixed demand.

c) Visual inspection.

Figure 6 illustrates the application of these procedures to streamflow in the Colorado River at Lees Ferry. In the first option a drought is defined as a consecutive series of years during which the average annual streamflow is continuously below some specified threshold level, which is typically taken to be the long term mean (Dracup et al., 1980; Yevjevich, 1967; Kendall and

Dracup, 1991a). These periods are termed hydrologic droughts. A hydrologic drought can be defined by the following three attributes:

(1) Duration (L).

(2) Deficit magnitude (M). The cumulative deficit below the threshold.

(3) Deficit intensity. The average deficit below the threshold (M/L).

Tables 2 to 5 list the droughts with large deficit magnitude in each streamflow series. The mean was used as the threshold for drought identification. A drawback of this procedure is that is classifies separately droughts that occur in quick succession separated by a single wet year (greater than the mean flow) that is insufficient to fill reservoirs.

Option (b), storage deficit analysis (also referred to as the sequent peak procedure (Kendall and Dracup, 1991b)) is a procedure whereby the storage deficit in a hypothetical semi-infinite reservoir initially full (zero deficit) is computed. Change in deficit is calculated each year using a constant yield (taken to include outflow as well as evaporation) minus the inflow. If the deficit ever becomes negative the excess is assumed to spill and deficit is reduced to zero. The maximum deficit is theoretically the storage capacity required to support the specified outflow or yield. In Figure 6d the yield was taken as 98% of the mean annual reconstructed streamflow (13.26 MAF), to reflect a high level of development. This high utilization is what is projected for the Colorado River in the year 2020 and is best for identification of sustained critical periods. An advantage of this analysis is that it gives an idea of the time required for a highly developed system with large storage to recover from a drought. Two or more droughts separated by a few wet years will still appear as critical in this analysis, if the intervening wet years are insufficient for the system to fully recover. As represented here this is simply a drought identification tool and only very roughly represents what may happen to reservoir storage during a severe sustained drought. In times of severe drought the demand is elastic and as deficits increase the demand will start to be curtailed through publicity campaigns, rationing etc.

Considering all of this information the most critical period in the Colorado River basin was the years from 1579-1600 which contained three hydrologic droughts in quick succession (Figure 6b) and represented the most rapid increase in deficit (Figure 6d.). By comparison the largest deficit in Figure 6d accumulates over 150 years, too long a period to consider as a single drought event for this study. However this does indicate that as the demand approaches the mean flow, very long (150 year) periods with no surplus are possible. Similarly, the period from 1918-1939

in California is characterized by a quick succession of hydrologic droughts and a sharp increase in the storage deficit (see Figure 7) to a maximum deficit of more than 60 MAF. This critical period is in recorded history, negating the necessity to use tree ring reconstructions to determine the most severe drought in California. This deficit accumulates over 20 years (1918-1937) and is roughly double the deficit accumulated during the recent California drought (1987-1991). Within the period (1918-1939) there is a 5 year period (1928-1932) that has an accumulated deficit of 35.6 MAF, slightly more severe than the 1987-1991 drought that which an accumulated deficit of 34.6 MAF. (These deficits are from the storage deficit analysis with yield taken as 98% of the mean, and therefore differ numerically from those reported in Table 4 which gives deficit below the mean.)

The following drought scenarios were identified and used in this study.

1. Colorado Severe Drought. The Colorado River drought of 1579 to 1600 as reconstructed from tree rings.

2. California Severe Drought. The drought of 1918 to 1939 in the historic unimpaired streamflow record.

3. Colorado Drought of Historic Record. The drought of 1943 to 1964 in the historic unimpaired streamflow record.

Droughts 2 and 3 are defensible as likely to recur, not withstanding any doubt surrounding the reliability of the tree ring reconstructions. It was also desired to have a drought scenario that would tax the system beyond its limits, which was defined as follows:

4. Colorado Rearranged Severe Drought. The Colorado River drought of 1579 to 1600 with annual flows re-arranged to be in descending order in this period. This makes the same amount of water available as in scenario 1, but the extremely low flows are clustered together at the end, when reservoirs are already low or dry. This drought is illustrated in Figure 8.

In the section below on quantification of drought risks the risk (return period) associated with each of these scenarios is estimated. The likelihood of joint occurrence of these drought scenarios in California and the Colorado River basin is discussed.

Spatial Variability and Disaggregation

One goal of this project is to focus on the geographic impact of drought and the ability of the water management infrastructure and institutions to equitably and efficiently distribute the water that is available. This requires knowledge of the spatial distribution of water for the drought

scenarios studied. Models of the water demand and allocation systems, such as the Colorado River Simulation System and California Department of Water Resources model, require monthly inputs at spatially distributed source points. Flows reconstructed from tree rings are aggregate values representing the sum of flows from all sites and seasons. To use these flows for drought planning requires that they be disaggregated into flows at each source site for each season (month). Procedures that are well documented and researched (Bras and Rodriguez-Iturbe, 1985; Grygier and Stedinger, 1988; Loucks et al., 1981; Salas et al., 1980; Stedinger et al., 1985; Stedinger and Vogel, 1984) are available for disaggregation of annual basin aggregate flow into monthly flow at each site.

Here, disaggregation procedures were applied to drought scenarios 1 and 4 developed above. These provide reasonable estimates of possible spatial configurations of a drought scenario that has been defined by an aggregate Lees Ferry flow. Drought scenarios 2 and 3 were in the historic record and their spatial configuration was already known. Estimated historic unimpaired flows at source locations were used in the study of these scenarios.

The basic idea is to subdivide the annual streamflow at a downstream site, such as Lees Ferry into streamflow at the individual upstream sites while retaining the cross correlations between flows at each site and autocorrelation between streamflow in different months. This method was applied to the twenty nine source locations identified in Figure 1. Where these source locations are downstream of other source locations the source streamflow is defined as the gain (or loss) in streamflow, calculated as streamflow at the given location minus streamflow from the upstream locations. With this convention where there are instream losses the source streamflow may be negative. The cross correlation between annual flows at all sites was computed and very strong cross correlations, defined by cross correlation ρ greater than 0.8 are shown in Figure 9. This figure shows that there is a strong spatial pattern to the correlation structure of streamflow in the Colorado River basin. Three distinct groups are apparent: (i) Streamflow originating in the Colorado Rocky mountains (Sites 4, 8, 9, 10, 12, 13, 14, 15). (ii) Streamflow originating in the Uinta mountains (Sites 3, 5, 6, 7, 30) with the upper reaches of the Green River (Sites 1 and 2) included for completeness. (iii) Streamflow originating in southern Colorado and northern New Mexico in the San Juan and Dolores Rivers (Sites 17, 18, and 19) with gains in the Colorado River main stem and the Paria River (Sites 16, 20, and 21) included to complete the upper basin. The inter correlation between flows originating in the lower basin (downstream of Lees Ferry) is not

nearly as strong. This grouping was used to determine the "staging" of the disaggregation procedure, according to Figure 10. Staging is used to reduce the size of the covariance matrices and number of model parameters to manageable numbers. Without staging, direct disaggregation into 29 sites and 12 months would require 121,104 cross correlations to be reproduced. This is more than the number of flow values to calibrate against (78 yrs x 12 months x 29 sites = 27,144 data) so is an inherently ill posed problem. With the staging shown in Figure 10, the number of cross correlations directly reproduced are 2,748, a much more manageable figure, given the amount of data.

The statistical streamflow disaggregation package SPIGOT (Grygier and Stedinger, 1988; 1990a; 1990b) was used to do the disaggregation. This was modified to disaggregate flows using the tree ring reconstructed records as aggregate flow, instead of generating the aggregate annual flow with an auto-regressive order one process. Stedinger [personal communication, 1991] assisted with this modification. SPIGOT was also modified to run on a UNIX workstation, which enabled the large runs necessary for a basin of this size to be completed in a few minutes of execution time.

The strategy of SPIGOT is first to disaggregate the annual flows at the aggregate site into monthly flows, and then to disaggregate these spatially. This has the effect of directly preserving monthly autocorrelations at the aggregate site and spatial cross correlations within each month. The monthly autocorrelation at each site is not directly preserved, instead it is approximated through modeling the autocorrelation of the residuals (Stedinger and Vogel, 1984). The annual spatial cross correlations are not directly preserved, but should be approximated well if each month is modeled well. Even though not directly modeled the annual spatial cross correlations were generally well reproduced in this study, as is shown below.

In any stochastic modeling of streamflow, fitting the marginal probability distribution used to represent the flow at each site in each month is important. SPIGOT gives four choices for this: Normal, two parameter log-normal, three parameter log-normal and approximated three parameter gamma or Pearson type III distributions. The parameters are estimated by matching moments and the best fitting of these, as measured by the correlation of observations with the fitted distribution quantiles (Filliben's correlation statistic, Grygier and Stedinger 1990b) is used as a marginal distribution. Where the normal distribution fits best no transformation is required. In the case of log-normal distributions the following equation is used to normalize the streamflow.

$$X_t = \ln(Q_t - a) \tag{1}$$

The shift parameter, a, is zero for the two parameter log-normal distribution. In the case of the approximated gamma distribution the Wilson-Hilferty transformation (based on Loucks et al., 1981, p.286) is used.

$$X_t = \frac{6}{\gamma_Q}\left(\left[\frac{\gamma_Q}{2}\left(\frac{Q_t - \mu_Q}{\sigma_Q}\right) + 1\right]^{1/3} - 1 + \frac{\gamma_Q^2}{36}\right) \tag{2}$$

Here Q_t is the observed streamflow, μ_Q the observed mean, σ_Q the observed standard deviation and γ_Q the observed skewness. X_t has a standard normal distribution. The best fitting transformation is applied to each month at each site so that the disaggregation can be done in a normalized or transformed variable space. Thus it is actually the statistics of the normalized flows that will be directly reproduced rather than the statistics of the actual flows which are only approximated. Procedures exist for incorporating skewness into disaggregation models but these are problematical (Lettenmaier and Burges, 1977). Stedinger and Vogel (1984) recommend the procedure used, namely first developing a satisfactory marginal distribution of the individual series and then using this to transform the flows. It was considered important to fit the marginal distributions well, especially for low flows, so I used Nonparametric procedures to plot and compare the estimated, fitted and simulated distributions. These procedures are described in detail in the Appendix. The results shown below indicate that despite the distribution choices available it is sometimes hard to fit the observed data well and a wider choice of distributions or the use of nonparametric distributions may be worthwhile in the future.

The annual to monthly disaggregation model used in SPIGOT is the condensed model described by Grygier and Stedinger (1988; 1990a; 1990b):

$$X_i = \alpha_i + \beta_i Y + \gamma_i X_{i-1} + \delta_i \sum_{j=1}^{i-1} w_j X_j \tag{3}$$

where Y is the normalized annual flow, X_i the normalized flow in month i, w_i a set of weights

dependent on the marginal distribution used, chosen to maximize the likelihood of the untransformed monthly flows adding to the untransformed annual flow. α_i, β_i, γ_i and δ_i are parameters estimated by regression for each month. For the first month, δ_i is constrained to be 0 and for the first two months γ_i is constrained to be 0 to ensure self consistency in the sense discussed by Stedinger and Vogel (1984).

The spatial disaggregation model used is described by Stedinger and Vogel (1984):

$$\mathbf{X}_i = \mathbf{B}_i \mathbf{X}_{k_i} + \mathbf{V}_i \tag{4}$$

where X_{k_i} is the normalized (zero mean) flow at the aggregate or key site in month i, X_i is a vector of normalized (zero mean) flows at disaggregated sites in month i, B_i is a vector of parameters and V_i a vector of zero mean random inputs at each site in month i. These inputs are independent of processes $\mathbf{X}_i$ and X_{k_i} but can be cross-correlated and have serial correlation themselves. In SPIGOT, to save on the number of parameters, the $\mathbf{V}_i$ are modeled as auto-regressive order-one processes at each site with no cross-correlation (Grygier and Stedinger, 1990a). This has the effect of representing some of the monthly autocorrelation at each site that is not directly reproduced, while leaving the representation of cross-correlation to come through the relationship to the aggregate or key site. The parameters for the spatial disaggregation model are estimated from sample moments of the observed normalized flows.

Verification of the SPIGOT model

SPIGOT provides a verification module to test the flows generated. For a basin the size of the Colorado River basin, and considering the number of sites modeled, this module produces an enormous amount of printed output that is hard to evaluate. Graphical procedures were therefore developed to test and validate the simulated flows. These are illustrated below. Once the model structure had been defined and parameters estimated, 10 simulations each of length 80 years were run. The length of 80 was chosen to be close to the length of the recorded streamflow record (78 years) and the number 10 is arbitrary. The aggregate series was taken as an 80 year subset of the 442 year Lees Ferry streamflow reconstruction as follows:

Years	Simulation
1550-1629	1, 6
1630-1709	2, 7
1710-1789	3, 8
1790-1869	4, 9
1870-1949	5, 10

The marginal probability distribution for each site and each month was estimated from the recorded flows using the non-parametric techniques described in the Appendix and compared to the fitted SPIGOT distribution and distribution estimated from each of the 10 simulations (Figure 11). A box plot technique is used to display the range over which the probability density estimated for the simulations varied. Boxes extend over the middle half of the data, with whiskers extending out a span 1.5 times the interquartile range. Occasional data beyond the span of the whiskers is plotted as dots. The historic data, upon which the solid line probability density estimate is based, is plotted as dots along the x-axis.

Each simulation is by construction a sample from the model probability distribution. Since the simulations had length (80 years) close to the length of the observed record the spread indicated by the boxes indicates the sampling uncertainty associated with the statistic plotted (in this case sample probability density). Where the boxes span a range that includes the estimate based on observed flows, one can attribute differences between observed and simulated statistics to sampling error. However, when the estimate based on observations falls outside the boxes, it indicates differences between model simulations and observations that cannot be explained as due to sampling effects and is model bias or error. Figures 11a and b show examples of the better fits obtained. These are typical of most distribution fits. Figure 11c shows a case where the historic data appears bimodal and this is not captured by the fitted log normal distribution so is not reflected in the simulations. In Figure 11d the historic data is partially bimodal. This is not reproduced by the Log normal distribution. Also in this Figure the simulations deviate from the fitted distribution. In this case we believe this is due to adjustments to make disaggregate flows add to aggregate flows introducing some bias. Figure 11e shows a case where the historic distribution is peaked with fat tails. The choices of distributions in SPIGOT could not fit this well. This was fairly often the case in gain sites where negative flows (infiltration losses) exist in the data. Figure 11f gives

an example of where the fitted distribution cut off sharply above an apparent lower bound. The non parametric density estimated from observed data and simulations do not show this sharp cutoff. This is boundary effect bias in the non parametric density estimation procedure caused by the kernels placed on top of boundary points extending beyond the domain boundary.

The observed mean and standard deviation (Figure 12) and 10% and 90% quantiles (Figure 13) of flows at each site in each month were also compared to the simulations. The mean and standard deviations fit well in all cases, however there were some discrepancies in the quantiles for sites where the marginal distribution fit was not good.

Figure 14 gives examples of the plots used to check the reproduction of autocorrelations at each site. The monthly and annual autocorrelations for lags 1 to 4 for the recorded flows (solid line) and range of simulations (boxes) were plotted. Except for the aggregate site (Lees Ferry) the disaggregation model does not directly reproduce month to month correlations, instead these are approximated by building a correlation structure into the innovations process (V in equation (4)). The reasonable fits obtained here demonstrate how well this works. Note that the lag one correlation in the first month of the water year is never reproduced. This represents the cross year correlation between the first month of one year and the last month of the previous year. It is a drawback of disaggregation models that the cross year correlations are not reproduced. Ideally, to minimize the effect of this, the start of the water year should be chosen as the month that has lowest correlation with flows in the previous month. Here this was not possible because the aggregate tree ring reconstructed flows were for the standard October to September water year. Due to this effect the first two lag two, first three lag three, and so on, correlations are also not reproduced.

To check the representation of site to site cross correlations the cross correlation between monthly and annual flows for each possible site pair was plotted. Figure 15 illustrates some of these with the solid line representing observed flows and the boxes the range of the simulations. Site to site monthly cross correlations between sites in different groups (such as sites 1 and 4) are not directly reproduced but approximated through the correlation between the key sites they are subservient to. Also annual cross correlations are not directly reproduced but well approximated by the monthly cross correlations being simulated.

These plots were used to refine the disaggregation staging structure and marginal distribution selected at each site and in the final run to verify that the model was performing satisfactorily.

In early runs of the model, we experienced problems with sometimes large negative flows being generated at sites 2, 16 and 20. This was traced to be due to the procedure that adjusted subservient flows to sum to the aggregate, which failed because negative flows (infiltration losses) are permissible at source locations 2, 16 and 20. To circumvent this problem, we generated flow at locations 2 and 3 combined, and locations 16, 20 and 21 combined (see Figure 9). These were then split proportionally to their historic mean flows rather than using a statistical disaggregation model. Flows at these sites are, therefore not correctly correlated with other flows, but since they are so small the error introduced is negligible.

Possible Spatial manifestation of drought scenarios 1 and 4.

Once the SPIGOT model and parameters had been verified, we generated twenty simulations using the ring reconstructed flow at Lees Ferry from 1570 to 1629. These years include the Colorado severe drought identified above, with sufficient time after the drought for system recovery. Each simulation represents a plausible spatial and monthly disaggregation of the tree ring reconstruction upon which it is based. These 20 simulations were then routed through the Colorado River system operations model, by other members of the study team and used for further drought planning and impact analysis. One simulation using the re-arranged aggregate flows (scenario 4) was also generated and used by the team in further analysis.

Quantification of drought risk for the study scenarios

This study used tree ring reconstructions of past streamflow to develop scenarios that had some physical basis. Here statistical techniques are used to assess the probability or risk of the drought scenarios developed. This information is necessary so that planners can be aware of the likelihood of the scenarios studied, or similar scenarios actually occurring. The evidence from geophysical data is that nature is continually changing with cycles of variability that stretch across years, decades and even millennia. The assumption that has to be made in quantifying the risk associated with future droughts is that the past is an indicator of the future. One has to assume stationarity and hope that the observed variability of the data about an average is large when compared to the long-term shifts in that average value. This can not be verified. Models that account for this uncertainty, such as models 3 and 4 below allow us to hedge our bets. However any planning that makes use of this information needs to recognize the inherent uncertainty in

planning for the future.

The basic statistics of the streamflow series studied were given in Table 1. The lag 1 correlation for historic unimpaired flows at Lees Ferry and the California four rivers is not significantly different from 0 at the 95% confidence level under a statistical hypothesis test based on the variance of the sample correlation (Bras and Rodriguez-Iturbe, 1985, p57). This may be due to the shortness of the record, but can be used to argue against using models with any sort of dependence between annual flows.

The Hurst coefficient has been estimated through rescaled range analysis (Pegram et al., 1980; Bras and Rodriguez-Iturbe, 1985; Feder, 1988). Range is defined as the maximum minus minimum cumulative departure from the mean in a sequence of flows n years long. Rescaled range is range divided by standard deviation. The Hurst coefficient is defined as the scaling exponent associated with the increase in rescaled range with sample size n.

$$C_t = \sum_{t=1}^{n} (Z_t - \overline{Z}) \tag{5}$$

$$\left(\underset{t\in(1,n)}{\text{Max}} (C_t) - \underset{t\in(1,n)}{\text{Min}} (C_t) \right) / \sigma_z^2 \sim n^H \tag{6}$$

It is recognized that given the length of record this is a highly uncertain statistic.

The likelihood of drought has been evaluated using four models for annual streamflow: (1) Independent annual flows; (2) Autoregressive order one model with fixed parameters; (3) Autoregressive order one model, allowing for parameter uncertainty; and (4) Fractional Gaussian noise model using the estimated Hurst coefficient. These cover the range of models that may be considered reasonable to simulate annual streamflow.

The extremely severe drought in the Colorado River from 1579 to 1600 was characterized by a sharp drop in the storage deficits and cumulative departure from the mean because the 17 year mean streamflow (1579 to 1595) is 10.47 MAF, and the 22 year mean streamflow (1579 to 1600) is 11.05 MAF, both figures being considerably less than the historic mean of 15.2 MAF, and tree ring reconstruction mean of 13.5 MAF. The California Severe drought is characterized by a 21 year mean of 13.72 MAF. The Colorado rearranged severe drought (see Figure 8) consists of 16 years with below mean streamflow and is characterized by a 16 year mean of 9.57 MAF.

The basis for assessment of the likelihood of these scenarios was to compute the probability and return period of mean flows below these thresholds for each of the models considered. The approach taken here is different from that of Loaiciga et al. (1992; 1993) who used renewal theory to analyze hydrologic drought (sequences of years with streamflow below a threshold). Here droughts are characterized by a mean streamflow below a threshold. This approach is more appropriate where there is large storage, such as in the reservoirs on the Colorado River. A single slightly above threshold wet year does not replenish storage and end drought.

Statistically the concept of return period, or recurrence interval, is well understood when talking about instantaneous occurrences. However care is needed when the occurrences of interest (droughts) are of significant length. In terms of instantaneous occurrences if the probability of an event in a unit time period is P, the return period is 1/P, measured in unit time periods. Now consider a multiple year event, such as an N year drought. Denote the probability of any N year period being such a drought as P_N. The return period measured in N year intervals is $1/P_N$, or measured in years is $R = N/P_N$. The probability of any one year being in an N year drought is $N/R = P_N$. Note that since P_N is a probability (less that 1) it is impossible to have R less than N, the duration of the drought being considered.

Tables 6 and 7 summarize calculations of return period R for each of the drought scenarios developed, using each of the annual streamflow models considered. Models 1 and 2 can be solved analytically so the results given are exact. Models 3 and 4 were solved by Monte Carlo techniques, simulating 10,000 years of streamflow.

Model 1. Independent Annual Flow

This model can be justified using the argument that autocorrelation between flow in different years is not statistically significant for the unimpaired streamflow data. Streamflow each year is assumed to be from a normal distribution independent of other years. Mean μ and standard deviation σ are taken equal to the sample values in Table 1. The variance of the N year mean is:

$$\sigma^2_{\bar{X}} = \frac{\sigma^2}{N} \tag{7}$$

A standardized normal distribution quantile q corresponding to the required threshold t_r is:

$$q = \frac{t_r - \mu}{\sigma_{\bar{X}}} \tag{8}$$

The probability p corresponding to quantile q is then obtained from normal distribution tables. This is the probability of an N year mean being less than the specified threshold. The return period is therefore N/p.

Model 2. Autoregressive order one model with fixed parameters.

An AR(1) model is written:

$$Z_t = \phi Z_{t-1} + \sigma_a W_t \tag{9}$$

Z_t is centered (mean subtracted) flow in year t, and W_t is an independent normally distributed unit variance random variable. The parameters ϕ and σ_a are taken as fixed at their maximum likelihood estimates: $\phi = \rho_1$, the lag one correlation and $\sigma_a^2 = (1 - \rho_1^2)\,\sigma_z^2$. This model has serial correlation ϕ^τ at lag τ. The N year moving average of serially correlated random variables has variance (Bras and Rodriguez-Iturbe, 1985):

$$\sigma_{\bar{X}}^2 = \frac{\sigma_z^2}{N}\left[1 + 2\sum_{\tau=1}^{N-1}(1-\tau/N)\phi^\tau\right] \tag{10}$$

This is used in equation (8) above to get the standardized variable corresponding to the specified threshold, and then from normal distribution tables we obtain p and the return period is N/p as before.

Model 3. Autoregressive order one model with uncertain parameters.

The importance of accounting for parameter uncertainty in streamflow models is noted by Loucks et al. (1981) and Grygier and Stedinger (1990a) describe how AR(1) model parameters can

be simulated based on their sample values and sampling uncertainty. When sample variance s^2 is estimated from the historical data, $\nu\, s^2/\sigma_z^2$ has a Chi-squared (χ^2_ν) distribution with $\nu = n-2$ degrees of freedom. n is the number of years of data used to estimate parameters. An AR(1) model with uncertain parameters is written:

$$Z_t = \alpha + \beta Z_{t-1} + \sigma_a W_t \tag{11}$$

α accounts for uncertainty, or differences between the sample mean, used to center the data, and population mean. Following Grygier and Stedinger (1990a) α is simulated from a normal distribution with mean zero (sample variance centered data) and variance 1/n. Simulation from a χ^2_ν distribution is then used to give σ_z^2 equal to $\nu\, s^2/\chi^2_\nu$. The value of β conditional on σ_z^2 is normally distributed with mean ρ_1 and variance $\sigma_z^2/(n\, s^2)$. The variance of the random component is then calculated as $\sigma_a^2 = (1-\beta^2)\,\sigma_z^2$. The probability and return period associated with critical periods defined by an N year mean less than a threshold is estimated by simulating 100 sets of parameters. Each set of parameters is then used to generate 100 years of streamflow resulting in a total of 10,000 years of simulated streamflow. 10,000 divided by the number of occurrences of droughts with N year mean less than a threshold gives a Monte Carlo estimate of the return period.

Model 4. Fractional Gaussian noise.

Models 1 to 3 assumed that streamflow is stationary with finite correlation scale. It has long been recognized that non stationarities, trends or periodicities at time scales longer than the observed data, or infinite memory and self similarity in streamflow series can lead to data that have Hurst coefficient H different from the theoretical asymptotic value of 0.5 for stationary finite correlation scale processes (Klemes, 1974; Mandelbrot and Wallis, 1969; Mandelbrot and van Ness, 1968; Bras and Rodriguez-Iturbe, 1985). It has also been established (Pegram et al., 1980; Feder, 1988) that records of the order of 100,000 data points are required for some stationary finite correlation scale models to converge to H = 0.5, making the question of whether H is really different from 0.5 philosophical rather than practical. Nevertheless the risk of severe drought using a fractional Gaussian noise model is evaluated.

The successive random addition procedure (Voss, 1985; Feder, 1988) was used to generate fractional Gaussian noise, with the same exponent H as estimated from the historical series. This method is very similar to the broken line process (Bras and Rodriguez-Iturbe, 1985; Curry and Bras, 1978). The starting point is a sequence of three positions $X(t_1)$, $X(t_2)$, $X(t_3)$, chosen from a normal distribution with zero mean and unit variance $\sigma_1^2 = 1$. The midpoints between these values are then estimated by interpolation and all positions are given a random addition with zero mean and reduced variance $\sigma_2^2 = (1/2)^{2H} \sigma_1^2$. This procedure is then continued with variance at each step $\sigma_n^2 = (1/2)^{2H\,(n-1)} \sigma_1^2$ until sufficient points have been simulated. The process is then scaled and centered so as to have the same mean and variance as historic data. Series of length 10,000 were simulated in this way and 10,000 divided by the number of occurrences of droughts with N year mean less than a threshold gives an estimate of return period.

Risk assessment.

In evaluating the results in Tables 6 and 7, one needs to bear in mind that the return periods reported are for multiple year events. The probability of any one year selected at random being in that scenario is the scenario duration divided by return period. The scenarios studied, except for the rearranged severe drought, came from either the observed or tree ring reconstructed historic record.

The historic record drought in the Colorado (1943 - 1964) is from an 80 year record and the simplistic return period estimate of 80 years agrees well with model 3 and model 4 calculations. Models 1 and 2 which either do not reproduce correlation, or assume parameters are perfectly estimated seem to overestimate this return period. This is consistent with the lack of memory in these models. The streamflow mean used to characterize the historic record drought is only just less than the Stockton and Jacoby (1976) reconstruction mean. This explains why return periods only slightly longer than the drought scenario itself are obtained from model estimates based on fits to the tree ring reconstruction. The severe drought in the Colorado (1579-1600) is from a tree ring streamflow reconstruction 442 years long. Again the simplistic return period estimate of 442 years compares well with models 3 and 4, but models 1 and 2 estimate significantly longer return periods.

The California severe drought was from an historic record 86 years long. The simplistic 86 year return period estimate again corresponds well with models 3 and 4, but not models 1 and 2. The limitations of the California four rivers tree ring reconstruction of streamflow (Figure 2c), also manifested in a considerably reduced standard deviation of reconstructed when compared with observed streamflow (Table 1), results in overestimates of the return period associated with the drought scenario when it is used to estimate model parameters. The return period estimates based on models fit to the California four rivers tree ring reconstruction are therefore disregarded.

Overall it can be concluded that models 1 and 2 are biased in their estimate of return period, due to not considering parameter uncertainty and correlation in the case of model 1. Models 3 and 4 give comparable results, bearing out the idea that the Hurst phenomenon which was reproduced by model 4 is equivalent to uncertainty in the underlying process parameters and possible non stationarity of these parameters that can not be resolved given the amount of data available. Risk assessment is based primarily on models 3 and 4. The following are proposed as reasonable estimates of the range of uncertainty associated with the return period of each scenario:

1. Colorado Severe Drought (1579-1600): 400 to 700 years.
2. California Severe Drought (1918-1939): 80 to 180 years.
3. Colorado Drought in Historic Record (1943-1964): 50 to 100 years.
4. Colorado Rearranged Severe Drought: 2000 to 10,000 years or more.

The ranges reflect uncertainty in these estimates. We believe that given the information at hand it is not possible to meaningfully reduce these ranges. Scenarios 2 and 3 are therefore once in a lifetime type occurrences, scenario 1 occurs less frequently and scenario 4, the rearranged drought is extremely rare, or even unrealistic.

Joint drought.

The possibility of joint occurrence of drought in the Colorado and California leading to additional hardship for communities that depend on both for water supply, such as the Los Angeles metropolitan area is of concern. The cross correlation between annual flow in the Colorado River at Lees Ferry and California four rivers index is 0.40, using the observed flows, 1906 to 1985, or 0.23 using the tree ring reconstructions (Stockton and Jacoby, 1976; Earle and Fritts, 1986) for the years of overlap, 1560 to 1961. These, although small, are statistically significantly different from zero. Loaiciga et al. (1992) also found a weak correlation of hydrologic conditions in California and Colorado river basins. For simplicity here we disregard this correlation and treat severe

sustained drought occurrence in the Colorado and California as independent processes. The risk of joint drought is therefore underestimated by the procedure given below.

Assume that droughts of durations T_1 and T_2, and return periods R_1 and R_2 occur independently in separate rivers. Define a joint drought as the overlapping in time, or concurrence of dht in each river. Then the probability of any one instant being in joint drought is the product of the individual drought probabilities, $\frac{T_1 T_2}{R_1 R_2}$. Given this, the probability of being at location (year) i of drought in basin 1 is uniform over the interval $0 < i < T_1$, with density $1/T_1$. Similarly the probability of being in location (year) j of drought in basin 2 is uniform over $0 < j < T_2$ with density $1/T_2$. The time from the start of joint drought is min(i,j) and the time to the end of joint drought is $\min(T_1\text{-}i, T_2\text{-}j)$. The duration of joint drought is:

$$L = \min(i,j) + \min(T_1\text{-}i, T_2\text{-}j). \tag{12}$$

Now evaluating the mean (expected value) of this over the joint density $\frac{1}{T_1 T_2}$, assuming without loss of generality that $T_2 \leq T_1$ we obtain:

$$E(L) = 2 + \frac{T_2^2}{3 T_1} - \frac{T_2}{T_1} \tag{13}$$

The recurrence interval of joint drought is therefore:

$$\frac{E(L)}{T_1 T_2 / R_1 R_2} = R_1 R_2 \left(\frac{2}{T_1 T_2} + \frac{T_2 - 3}{3 T_1^2} \right) \tag{14}$$

Table 8 gives the recurrence interval and expected duration of the California drought scenario with each of the Colorado River drought scenarios. This shows that the occurrence of joint drought in

California and the Colorado River of appreciable duration (> 5 years) is not significantly less frequent than the rarer of the individual scenarios. In particular the return period of joint California and Colorado historic record droughts is estimated to be only 130 years.

This analysis has assumed drought occurrence in the two regions to be independent and therefore this joint occurrence is due to coincidence. The weak correlation observed between streamflow in California and Colorado river basins, possibly due to climate system linkage, would increase the risk of joint drought.

Conclusions

Drought scenarios have been developed for the study of severe sustained drought in the Colorado River basin and California. These scenarios were based on estimated unimpaired and tree ring reconstructed streamflow. Some discrepancies between different streamflow reconstructions were noted. Stochastic disaggregation techniques were used to generate plausible spatial manifestations of severe sustained drought from drought scenarios defined in terms of Lees Ferry aggregate flows. Because of the size of this disaggregation problem visual graphical techniques, such as the boxplot and non parametric density estimate, were extensively used to validate the disaggregation model. A variety of stochastic models including independent, autoregressive order one and fractional Gaussian noise were used to estimate the return period and risk associated with the drought scenarios developed. The risk of joint occurrence of sustained drought in the Colorado River and California was also calculated and found to occur nearly as frequently as drought in either region considered separately. These occurrence risks should be borne in mind when evaluating and developing planning strategies based on these scenarios.

Appendix. Non parametric procedures for estimation of probability density functions

Crucial to this study and to many studies in hydrology is the estimation or fitting of a probability density function. Historically a common approach has been to select a particular distribution from a suite of choices (Normal, Log-normal, Gamma, Extreme value etc.) and estimate the parameters using one of a variety of statistical techniques (method of moments, maximum likelihood etc.). This approach is problematical because we can not in general know in advance what the right distribution is. In many cases the goodness of fit is illustrated by comparison to a histogram, the simplest non-parametric representation of a probability distribution. The philosophy of the histogram is simple. By counting the number of data points within a range and plotting a bar graph, one obtains an impression of the clustering or density of the data. Where the data is closely clustered probability density is high and where there is little or no data probability density is low. The drawback of a histogram is that it is sensitive to the width and positioning of ranges into which the domain is divided and data counted. Also it is discontinuous with jumps at range transitions. Non-parametric techniques using kernel density estimates have been developed (Silverman, 1986) to overcome some of these deficiencies. The purpose of this appendix is to describe the application of the non-parametric density estimator that we used to compare probability distributions. We also describe some adjustments made to account for the fact that some of the data used, although physically measurable as continuous, has been rounded and reported as integer valued data. The procedures we use are largely based on methods described in Silverman (1986).

A kernel probability density estimator is written

$$f(x) = \sum_{i=1}^{n} \frac{1}{n\,h_i} K\left(\frac{x-x_i}{h_i}\right) \qquad \text{(A-1)}$$

where there are n sample data x_i. K(.) is a kernel function that must integrate to 1 and h is a parameter called the band width that defines the spread of probability around each data point x_i. It is akin to the histogram bin width, in that if chosen too small it results in spikes at each data point, and if it is too large it blurs or oversmooths the resulting density estimate. Typical kernel functions are illustrated in Figure A-1. Through placing kernels on the data points themselves, one overcomes the criticism of the histogram, that it is position dependent; and by choosing continuous

kernel functions, that it is discontinuous. Band width, analogous to histogram bin width, needs to be narrow where the data is dense, but large where the data are sparse. This suggests data adaptive or variable band widths. We used

$$h_i = \alpha\, d_{k_i} \tag{A-2}$$

where α is an overall bandwidth scale parameter and d_{k_i} is the distance to the k'th nearest neighbor from point i. Following suggestions of Silverman (1986), the number of nearest neighbors, k, was taken as $n^{0.8}$ and the overall band width scale parameter α chosen so that mean band width is proportional to a robust estimator of standard deviation.

$$\alpha = 0.9\, n^{-0.2} \min\{\text{standard deviation, (interquartile range/1.34)}\} \tag{A-3}$$

Procedures similar to this have many pleasing theoretical and convergence properties that are discussed at length in the statistics literature. Refinements are continuously appearing. This procedure was implemented and used to plot probability density estimates for various individual month streamflows at source inflow locations. Typical results are illustrated in Figures A-2, together with fits of typical parametric distributions and histogram. The results are visually pleasing, in addition to the theoretically appealing lack of parametric assumptions and statistical convergence properties. The procedure is relatively insensitive to outliers and can represent skewness in the data well. There is no significant difference between the two kernels used. Silverman (1986) lists efficiency measures for each of these kernels that gives the Epaneckhnikov kernel a slightly higher rating, so we have chosen it for our work.

There is however a problem when the data are clustered on discrete integer values due to rounding. This is illustrated in Figure A-3. The estimated density has bumps over the integer data points. There is no physical reason for streamflow to assume integral values and the numbers reported could have been anywhere in the rounding range $(x_i - \delta, x_i + \delta)$, usually $\delta = 0.5$. To account for this we assume each x_i could be randomly located in the rounding range with a uniform probability distribution. The expected value of f(x) can then be evaluated by integrating over these distributions. The resulting estimator is then:

$$f(x) = \sum_{i=1}^{n} \frac{1}{n\,h_i} \int_{x_i-\delta}^{x_i+\delta} K\left(\frac{x-x_i}{h_i}\right) dx_i \qquad \text{(A-4)}$$

Effectively this amounts to modifying the kernel to also depend on δ. For a Gaussian kernel:

$$f(x) = \frac{1}{n} \sum_{i=1}^{n} \frac{1}{4\delta} \left[\operatorname{erf}\left(\frac{\delta-x+x_i}{\sqrt{2}\,h_i}\right) + \operatorname{erf}\left(\frac{\delta+x-x_i}{\sqrt{2}\,h_i}\right) \right] \qquad \text{(A-5)}$$

where erf(.) is the error function (gaussian integral) (Abramowitz and Stegun, 1972). For an Epanechnikov kernel:

$$f(x) = \frac{1}{n} \sum_{i=1}^{n} \left[\frac{3}{8\delta}\left(\frac{b-a}{h_i}\right) + \frac{1}{8\delta}\left(\frac{x-b}{h_i}\right)^3 - \frac{1}{8\delta}\left(\frac{x-a}{h_i}\right)^3 \right] \qquad \text{(A-6)}$$

where a and b are the limits over which the integral is non-zero (i.e. the data error range and kernel support overlap) and are:

$$a = \max(x - \sqrt{5}\,h_i,\ x_i - \delta) \qquad \text{(A-7)}$$

$$b = \min(x + \sqrt{5}\,h_i,\ x_i + \delta,\ a) \qquad \text{(A-8)}$$

Figure A-3 illustrates the results from applying this modification. In the results shown in Figure 11 this variable bandwidth kernel density estimator with rounding adjustment has been used as an empirical tool, analogous to plotting histograms, to compare the probability density derived from historical data to that derived from simulations and the theoretical distribution used in the simulations. The range of the distributions derived from simulations, illustrated with the box plots gives a measure of the uncertainty associated with applying this nonparametric density estimator with the given amount of data.

Acknowledgements

This research was supported by the U.S. Geological Survey (USGS), Department of the Interior, under USGS award number 14-08-0001-G1892, with matching support from the Metropolitan Water District of Southern California and Utah Water Research Laboratory. The views and conclusions contained in this paper are those of the author and should not be interpreted as necessarily representing the official policies, either expressed or implied, of the U.S. Government

L. Douglas James lead the severe sustained drought study team, set the direction and contributed ideas to this work. The work has benefited from discussion with members of the severe sustained drought study team and advisory panel, too numerous to mention. Jan Grygier made available source code for the SPIGOT model and Jery Stedinger suggested how it could be modified to work off tree ring reconstructed streamflow. The use of non-parametric distributions followed suggestions by Upmanu Lall. Ashish Sharma assisted with some of the risk calculations. The paper benefited from reviews by David Maidment, Upmanu Lall and an anonymous reviewer.

Table 1. Statistics of Streamflow Series

Series	Length (years)	Mean (MAF[1])	Standard deviation (MAF)	Lag 1 correlation	Hurst coefficient
Unimpaired flows at Lees Ferry 1906 to 1985	80	15.2	4.24	0.21*	0.73
Stockton and Jacoby (1976) Lees Ferry reconstruction	442	13.5	3.59	0.32	0.63
Michaelson et al. (1991) Lees Ferry reconstruction	395	13.8	3.61	0.26	0.65
California four rivers unimpaired 1906 to 1991	86	17.8	7.65	0.09*	0.67
Earle and Fritts (1986) California four rivers reconstruction	421	17.5	4.41	0.19	0.64

* Note: These correlations are not statistically different from 0 at the 95% confidence level.

1. MAF (million acre-feet) = acre feet x 10^6 = 1.23 x 10^9 m^3.

Table 2. Hydrologic Droughts in the Colorado River at Lees Ferry historic streamflow. Threshold (mean) = 15.2 MAF[1]. Droughts with deficit magnitude greater than 15 MAF.

	Duration (years)	Deficit Intensity (average deficit) (MAF)	Deficit Magnitude (accumulated deficit) (MAF)
1953-1956	4	5.0	20.0
1933-1937	5	3.3	16.5
1976-1978	3	5.1	15.4
1959-1961	3	5.1	15.3

1. MAF (million acre-feet) = acre feet x 10^6 = 1.23 x 10^9 m^3.

Table 3. Hydrologic Droughts in the Colorado River at Lees Ferry reconstructed streamflow (Stockton and Jacoby, 1976). Threshold (mean) = 13.5 MAF. Droughts with deficit magnitude greater than 15 MAF, or in critical period for storage.

	Duration (years)	Deficit Intensity (average deficit) (MAF)	Deficit Magnitude (accumulated deficit) (MAF)	
1772-1783	12	2.7	32.8	
1579-1581	3	3.2	9.5	} Critical period 1579-1595
1583-1587	5	4.5	22.6	
1590-1595	6	4.1	24.4	
1531-1535	5	4.0	19.9	
1845 -1847	3	6.3	18.8	
1878-1883	6	3.0	17.7	
1663-1668	6	2.9	17.4	
1684-1689	6	2.7	16.4	
1630-1632	3	5.5	16.4	
1544-1547	4	3.8	15.1	

Table 4. Hydrologic Droughts in the California four rivers historic streamflow. Threshold (mean) = 17.8 MAF. Droughts with deficit magnitude greater than 18 MAF.

	Duration (years)	Deficit Intensity (average deficit) (MAF[1])	Deficit Magnitude (accumulated deficit) (MAF)	
1917-1920	4	4.5	18.0	} Critical period 1917-1937
1923-1926	4	6.1	24.5	
1928-1937	10	5.5	55.4	
1987-1991	5	7.6	38.1	
1944-1950	7	4.1	29.0	
1976-1977	2	11.2	22.4	
1959-1962	4	4.8	19.0	

Table 5. Hydrologic Droughts in the California four rivers reconstructed streamflow. Threshold (mean) = 17.5. Droughts with deficit magnitude greater than 18 MAF.

	Duration (years)	Deficit Intensity (average deficit) (MAF)	Deficit Magnitude (accumulated deficit) (MAF)
1928-1939	12	6.1	72.8
1836-1849	14	3.1	43.8
1717-1724	8	4.2	33.9
1589-1595	7	4.6	32.4
1651-1655	5	5.1	25.6
1755-1760	6	4.2	24.9
1578-1584	7	3.2	22.1
1793-1795	3	6.7	20.2
1735-1739	5	4.0	19.9
1776-1780	5	3.8	19.2

Table 6. Colorado River Drought Risk Assessment

		Drought of Historic record (1943-1964) Scenario 3.	Reconstructed severe drought (1579-1600) Scenario 1.	Rearranged severe drought of 1579-1600 Scenario 4.
Characterizing flow	Mean (MAF[2])	13.43	10.47 or[1] 11.05	9.57
	Duration (years)	22	17 or[1] 22	16
		Return period (years)	Return period (years)	Return period (years)
Fitted to unimpaired historic flows	Model 1.	970	9.9×10^6	3.6×10^8
	Model 2.	422	2.2×10^5	3.4×10^6
	Model 3.	107	5,000	> 10,000
	Model 4.	83	645	2000
Fitted to Stockton and Jacoby (1976) tree ring reconstruction of streamflow	Model 1.	49	38,000	3.3×10^6
	Model 2.	47	2,500	29,000
	Model 3.	32	555	4,000
	Model 4.	32	526	2857

1. The reconstructed severe drought can be characterized by either a 17 year mean of 10.47 MAF or a 22 year mean of 11.05 MAF. The smaller return period (and corresponding higher probability) associated with these is reported here, because flow below either of these constitutes the drought scenario.

2. MAF (million acre-feet) = acre feet x 10^6 = 1.23 x 10^9 m^3.

Model 1. Independent annual flow; Model 2. Autoregressive order 1 with fixed parameters; Model 3. Autoregressive order 1 with uncertain parameters; Model 4. Fractional Gaussian noise.

Once model parameters are estimated using either the historic unimpaired or tree ring reconstructed streamflow they are used to estimate return period for drought scenarios derived from both historic unimpaired and tree ring reconstructed streamflow.

Table 7. California Four Rivers Drought Risk Assessment

		Severe drought in historic record. (1918-1939)
Characterizing flow:	Mean (MAF[1])	14.14
	Duration (years)	22
		Return period (years)
Fitted to unimpaired historic flows	Model 1.	1808
	Model 2.	1104
	Model 3.	188
	Model 4.	102
Fitted to Earle and Fritts (1986) tree ring reconstruction of streamflow	Model 1.	109,000
	Model 2.	13,200
	Model 3.	909
	Model 4.	1,111

1. MAF (million acre-feet) = acre feet x 10^6 = 1.23 x 10^9 m^3

Table 8. Joint Drought Risk Assessment

Drought Combination	Mean Duration (years)	Recurrence interval (years)
California scenario 2, $T_1 = 22$, $R_1 = 100$ and Colorado scenario 1, $T_2 = 22$, $R_2 = 500$	8.33	861
California scenario 2, $T_1 = 22$, $R_1 = 100$ and Colorado scenario 3, $T_2 = 22$, $R_2 = 75$	8.33	129
California scenario 2, $T_1 = 22$, $R_1 = 100$ and Colorado scenario 4, $T_2 = 22$, $R_2 = 4000$	5.2	5850

Figure Captions

Figure 1. Southwestern United States study area showing the river and water distribution systems involved. Numbered points are the source inflow locations used by the Colorado River simulation model.

Figure 2. Comparison of observed and tree ring reconstructed annual streamflow in million acre feet (MAF), (a) Lees Ferry reconstruction (Stockton and Jacoby, 1976); (b) Lees Ferry reconstruction (Michaelson et al., 1990); (c) California four rivers (American, Yuba, Feather and Sacramento) combined (Earle and Fritts, 1986). The solid line is a 1:1 line and ρ indicates cross correlation coefficient.

Figure 3. Time series of historic and reconstructed streamflow, (a) Lees Ferry ; (b) Four California rivers (American, Yuba, Feather and Sacramento) combined.

Figure 4. Ten year moving average of historic and reconstructed streamflow at Lees Ferry.

Figure 5. Streamflow cumulative departures from mean. a) Lees Ferry (with reference to mean of Stockton and Jacoby (1976) reconstruction, 13.5 MAF). b) Four California rivers combined.

Figure 6. Colorado River at Lees Ferry drought identification. a) Streamflow, annual and 10 year moving average. b) Critical period for storage. c) Hydrologic drought with largest deficit magnitude. d) Storage deficit with annual yield of 13.26 MAF (98% of tree ring reconstruction mean).

Figure 7. California four rivers storage deficits with annual yield of 17.12 MAF (98% of tree ring reconstruction mean).

Figure 8. Colorado rearranged severe drought.

Figure 9. Spatial pattern of cross correlation between annual source streamflow in the Colorado

River basin.

Figure 10. Structure of the disaggregation model for the Colorado system. Numbers refer to locations in Figure 1.

Figure 11. Comparison of selected observed, fitted, and simulated monthly flow probability distributions. The dots along the x-axis are the observed streamflow. The solid line is the non parametric estimate of observed probability density calculated using the kernel method described in the appendix. The dashed line gives the probability density function used in SPIGOT. The boxes give the range of non parametric estimate of probability density calculated from each of the 10 simulations.

Figure 12. Comparison of selected observed and simulated mean and standard deviation. The large black dot and solid line indicate the observed statistic (mean or standard deviation) and the boxes indicate the range of the simulated statistic from each of the 10 simulations. Source locations 1 and two are in the upper reaches of the Green River, see Figure 1.

Figure 13. Comparison of selected observed and simulated 10% and 90% quantiles (flows equalled or exceeded 10% and 90% of the time respectively).

Figure 14. Comparison of selected observed and simulated autocorrelations.

Figure 15. Comparison of selected observed and simulated cross correlations.

Figure A-1. Typical kernels for non parametric density estimation.

Figure A-2. Annual flow in the San Juan river (source location 18) a) Histogram and Kernel estimates of probability density indicating bimodality; b) Common distribution fits. The dots on the x axis are the original data on which this is based.

Figure A-3. Kernel density estimates where data has been rounded and recorded as integer values, with and without rounding correction. The data is December flow at source location 9, the Taylor

river.

References

Abramowitz, M. and I. A. Stegun, (Ed.) 1972. Handbook of Mathematical Functions. Dover.

Bras, R. L. and I. Rodriguez-Iturbe, 1985. Random Functions and Hydrology. Addison-Wesley, Reading, MA, 559 pp.

Brown, T. C., B. L. Harding and W. B. Lord, 1988. Consumptive use of Incremental Flows in the Colorado River Basin. Water Resources Bulletin, 24: 801-814.

Brown, T. C., B. L. Harding and E. A. Payton, 1990. Marginal Economic Value of Streamflow: A Case Study for the Colorado River Basin. Water Resources Research, 26(12): 2845-2859.

Cook, E. R. and L. A. Kairiukstis, (Ed.) 1990. Methods of Dendrochronology. Kluwer Academic, Boston, Mass.

Curry, K. and R. L. Bras, 1978. Theory and Applications of the Multivariate Broken Line, Dissaggregation and Monthly Autoregressive Streamflow Generators to the Nile River. Report No. 78-5, Technology Adaptation Program, MIT, Cambridge, MA.

Dracup, J. A., K. S. Lee and E. G. Paulson, 1980. On the Statistical Characteristics of Drought Events. Water Resources Research, 16(2): 289-296.

Earle, C. J. and H. C. Fritts, 1986. Reconstructing Riverflow in the Sacramento Basin Since 1560. Report to California Department of Water Resources, Agreement No. DWR B-55398. Laboratory of Tree Ring Research, University of Arizona, Tuscon.

Feder, J., 1988. Fractals. Plenum Press.

Fiering, M. B., 1967. Streamflow Synthesis. Harvard University Press, Cambridge, MA.

Fritts, H. C., 1976. Tree Rings and Climate. Academic, San Deigo, Calif.

Grygier, J. C. and J. R. Stedinger, 1988. Condensed Disaggregation Procedures and Conservation Corrections for Stochastic Hydrology. Water Resources Research, 24(10): 1574-1584.

Grygier, J. C. and J. R. Stedinger, 1990a. Spigot, A Synthetic Streamflow Generation Package, Technical Description, Version 2.5. School of Civil and Environmental Engineering, Cornell University.

Grygier, J. C. and J. R. Stedinger, 1990b. Spigot, A Synthetic Streamflow Generation Package, Users Manual, Version 2.5. School of Civil and Environmental Engineering, Cornell University.

Kendall, D. R. and J. A. Dracup, 1991a. An Assessment of Severe and Sustained Drought in the Colorado River Basin. Chapter 2 in Severe Sustained Drought in the Southwestern United States, Phase 1 report to the U.S. Department of State, Man and Biosphere program,

Kendall, D. R. and J. A. Dracup, 1991b. A Comparison of Index-Sequential and AR(1) Generated Hydrologic Sequences. Journal of Hydrology, 122: 335-352.

Klemes, V., 1974. The Hurst Phenomenon: A Puzzle? Water Resources Research, 10(4): 675-688.

Lettenmaier, D. P. and S. J. Burges, 1977. An Operational Approach to Preserving Skew in Hydrologic Models of Long-Term Persistence. Water Resources Research, 13(2): 281-290.

Loaiciga, H. A., L. Haston and J. Michaelson, 1993. Dendrohydrology and Long-Term Hydrologic Phenomena. Reviews of Geophysics, 31(2): 151-171.

Loaiciga, H. A., J. Michaelson, S. Garver, L. Haston and R. B. Leipnik, 1992. Droughts in River Basins of the Western United States. Geophysical Research Letters, 19(20): 2051-2054.

Loucks, D. P., J. R. Stedinger and D. A. Haith, 1981. Water Resource Systems Planning and Analysis. Prentice-Hall, Englewood Cliffs, NJ, 559 pp.

Maidment, D. R., (Ed.) 1993. Handbook of Hydrology. McGraw Hill.

Mandelbrot, B. B. and J. W. van Ness, 1968. Fractional Brownian Motions, Fractional Noises and Applications. SIAM Review, 10(4): 422-437.

Mandelbrot, B. B. and J. R. Wallis, 1969. Operational Hydrology Using Self-similar Processes. In J. Lawrence (Ed.), The Fifth International Conference on Operational Research, Venice, Tavistock publications, pp. 264-282.

Michaelson, J., H. A. Loaiciga, L. Haston and S. Garver, 1990. Estimating drought probabilities in California using tree rings. Completion report to California Department of Water Resources, Department of Geography, University of California, Santa Barbara.

Pegram, G. G. S., J. D. Salas, D. C. Boes and V. Yevjevich, 1980. Stochastic Properties of Water Storage. Hydrology Paper No. 100, Colorado State University, Fort Collins, Colorado.

Rodriguez-Iturbe, I., 1969. Estimation of Statistical Parameters of Annual River Flows. Water Resources Research, 5(6): 1418-1421.

Salas, J. D., J. W. Delleur, V. Yevjevich and W. L. Lane, 1980. Applied Modeling of Hydrologic Time Series. Water Resources Publications, Littleton, Colorado, 484 pp.

Silverman, B. W., 1986. Density Estimation for Statistics and Data Analysis. Chapman and Hall, 175 pp.

Stedinger, J. R., D. Pei and T. A. Cohn, 1985. A Condensed Disaggregation Model for Incorporating Parameter Uncertainty into Monthly Reservoir Simulations. Water Resources Research, 21(5): 665-675.

Stedinger, J. R. and R. M. Vogel, 1984. Disaggregation Procedures for Generating Serially Correlated Flow Vectors. Water Resources Research, 20(11): 47-56.

Stockton, C. W. and W. R. Boggess, 1979. Augmentation of Hydrologic Records Using Tree Rings. In The Engineering Foundation Conference, Improved Hydrologic Forecasting - Why and How, Pacific Grove, CA, March 25-30, ASCE, pp. 239-265.

Stockton, C. W. and G. C. Jacoby, 1976. Long-Term Surface-Water Supply and Streamflow Trends in the Upper Colorado River Basin Based on Tree-Ring Analyses. Lake Powell Research Project Bulletin, No. 18, National Science Foundation.

Stockton, C. W., D. Meko and W. R. Boggess, 1991. Drought History and Reconstructions from Tree Rings. Chapter 1 in Severe Sustained Drought in the Southwestern United States, Phase 1 report to the U.S. Department of State, Man and Biosphere program,

Thomas, H. A. and M. B. Fiering, 1962. Mathematical Synthesis of Streamflow Sequences for the Analysis of River Basins by Simulation. In A. Maass et al. (Ed.), Design of Water Resource Systems. Harvard University Press, Cambridge, MA, pp. 459-493.

Voss, R. F., 1985. Random Fractal Forgeries. In R. A. Earnshaw (Ed.), Fundamental Algorithms in Computer Graphics, NATO ASI Series. Vol. F17. Springer Verlag, Berlin, pp. 805-835.

Wallis, J., (Ed.) 1977. Climate, Climate Change and Water Supply. National Academy of Science Press, Washington, DC.

Yevjevich, V. M., 1967. Objective Approach to Definitions and Investigations of Continental Droughts. Hydrology Paper 23, Colorado State University, Fort Collins, CO.

Yevjevich, V. M., 1972. Stochastic processes in hydrology. Water Resources Publications, Fort Collins, CO.

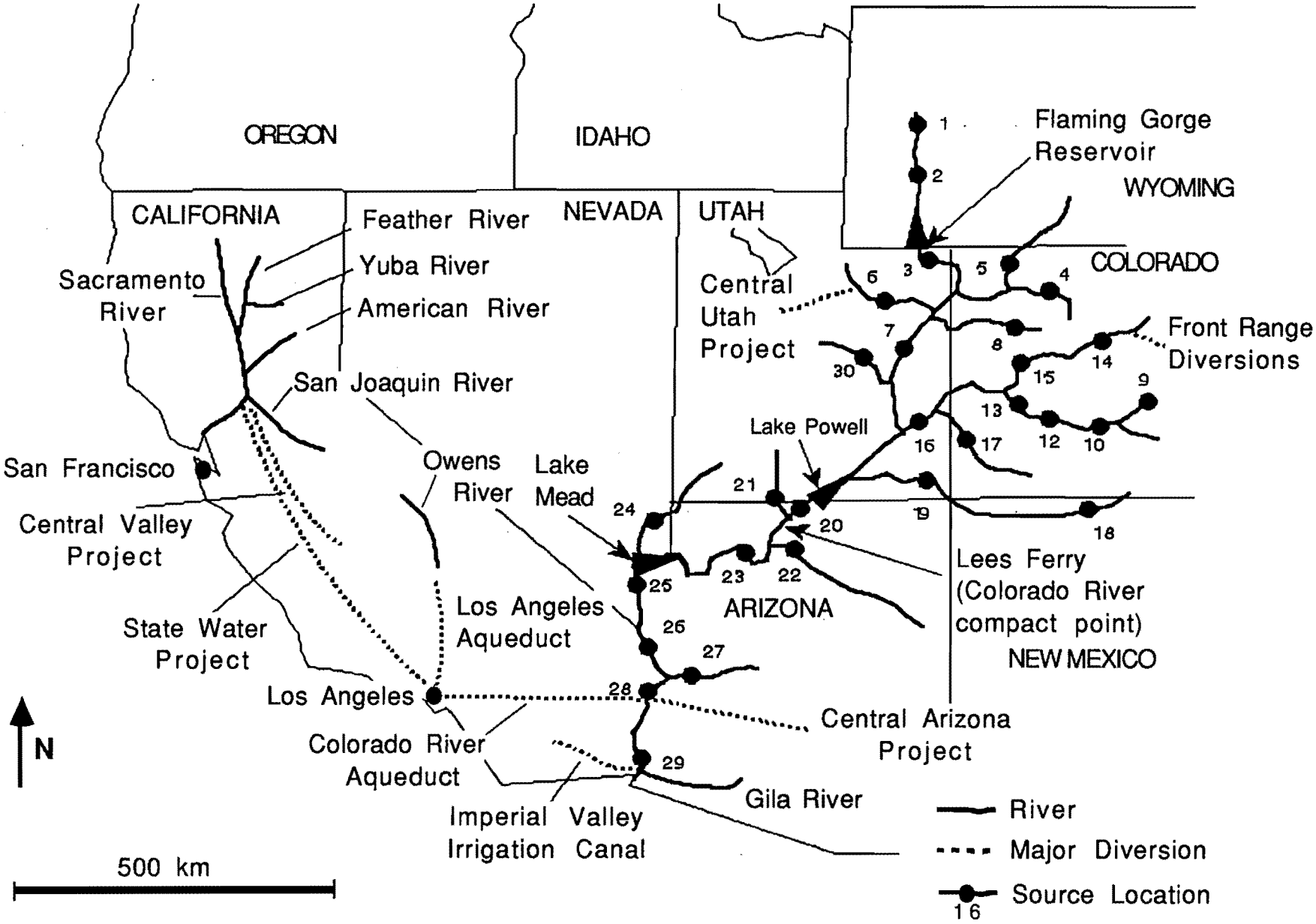
OREGON
IDAHO
CALIFORNIA
NEVADA
UTAH
WYOMING
COLORADO
NEW MEXICO
ARIZONA
Flaming Gorge Reservoir
Feather River
Yuba River
American River
Sacramento River
San Joaquin River
Central Utah Project
Front Range Diversions
Lake Powell
Lake Mead
Owens River
San Francisco
Central Valley Project
State Water Project
Los Angeles Aqueduct
Los Angeles
Colorado River Aqueduct
Imperial Valley Irrigation Canal
Gila River
Central Arizona Project
Lees Ferry (Colorado River compact point)
N
500 km
River
Major Diversion
Source Location
16

Figure 1.

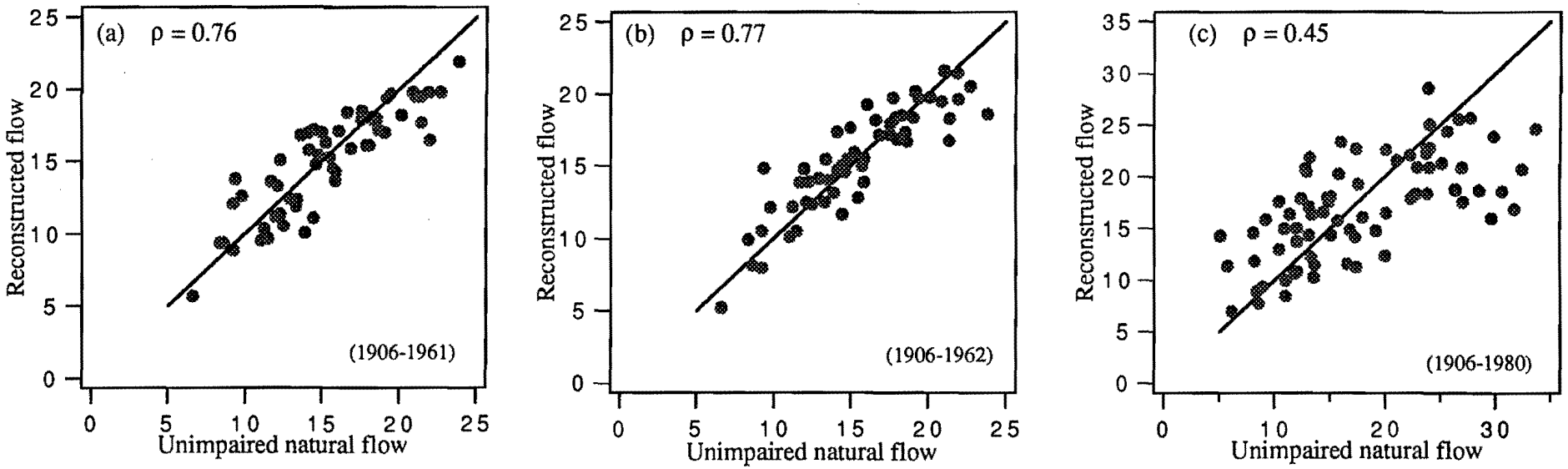
(a) ρ = 0.76
(1906-1961)
Reconstructed flow
Unimpaired natural flow
(b) ρ = 0.77
(1906-1962)
Reconstructed flow
Unimpaired natural flow
(c) ρ = 0.45
(1906-1980)
Reconstructed flow
Unimpaired natural flow

Figure 2.

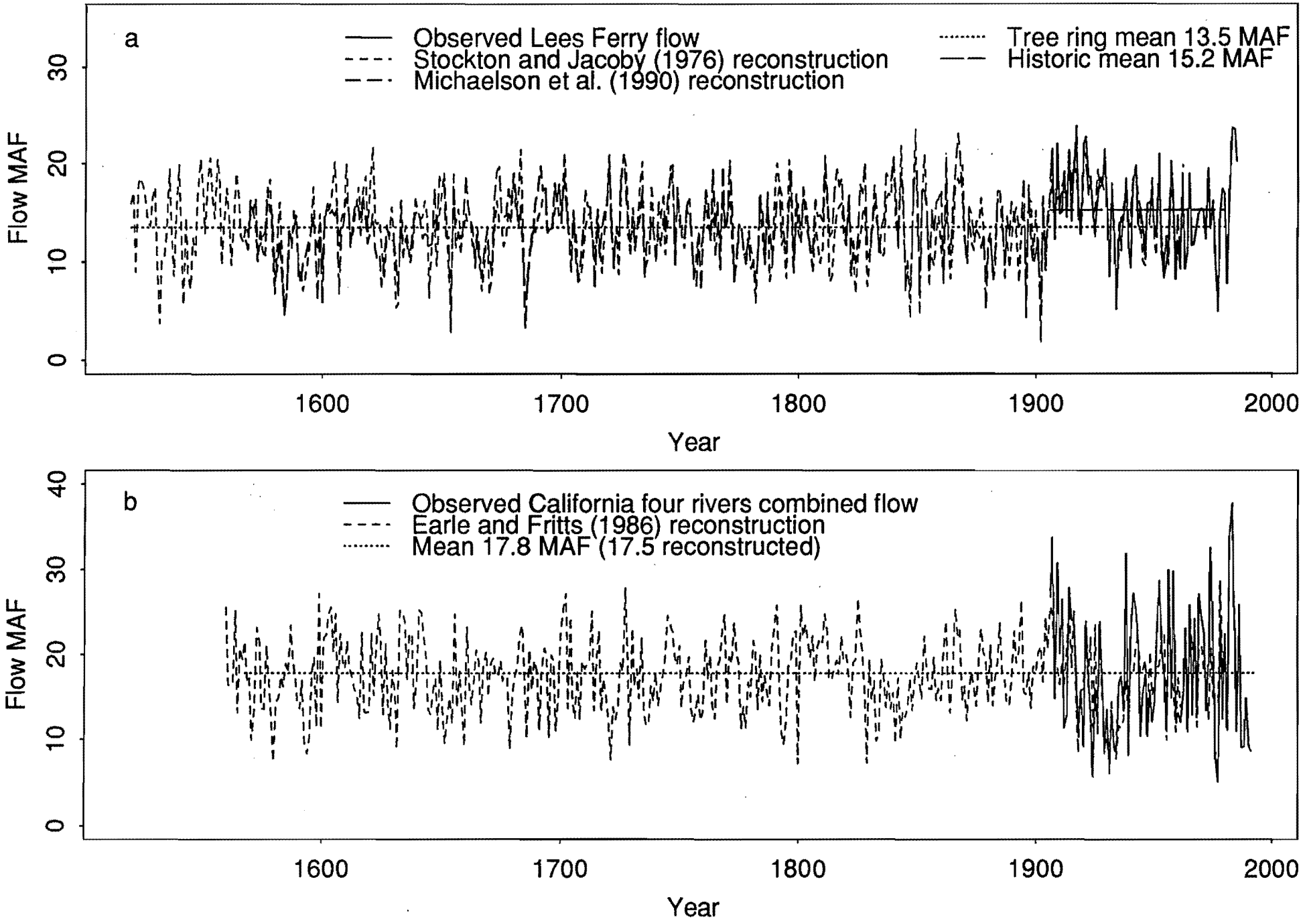
a
Observed Lees Ferry flow
Stockton and Jacoby (1976) reconstruction
Michaelson et al. (1990) reconstruction
Tree ring mean 13.5 MAF
Historic mean 15.2 MAF
Flow MAF
0
10
20
30
1600
1700
1800
1900
2000
Year
b
Observed California four rivers combined flow
Earle and Fritts (1986) reconstruction
Mean 17.8 MAF (17.5 reconstructed)
Flow MAF
0
10
20
30
40
1600
1700
1800
1900
2000
Year

FIGURE 3.

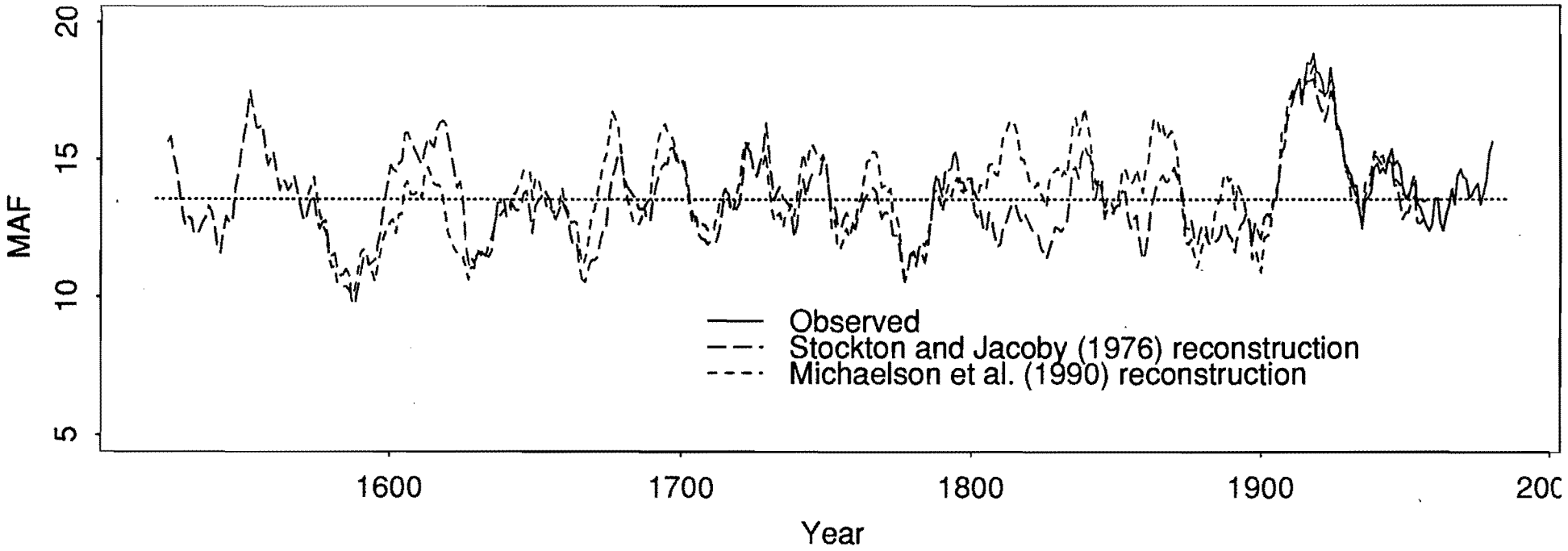
MAF
20
15
10
5
1600
1700
1800
1900
200
Year
Observed
Stockton and Jacoby (1976) reconstruction
Michaelson et al. (1990) reconstruction

FIGURE 4

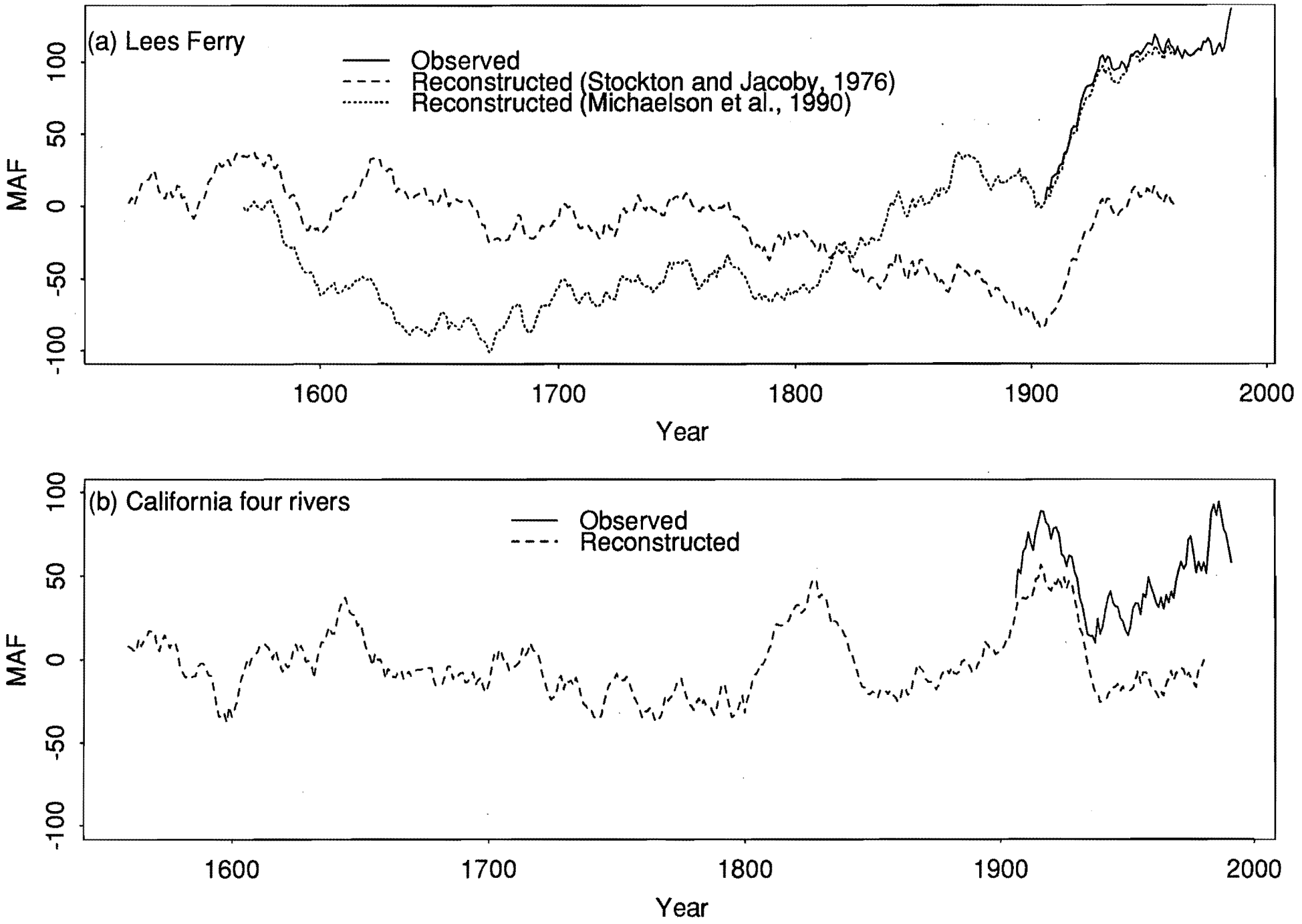
(a) Lees Ferry
Observed
Reconstructed (Stockton and Jacoby, 1976)
Reconstructed (Michaelson et al., 1990)
MAF
100
50
0
-50
-100
1600
1700
1800
1900
2000
Year
(b) California four rivers
Observed
Reconstructed
MAF
100
50
0
-50
-100
1600
1700
1800
1900
2000
Year

FIGURE 5

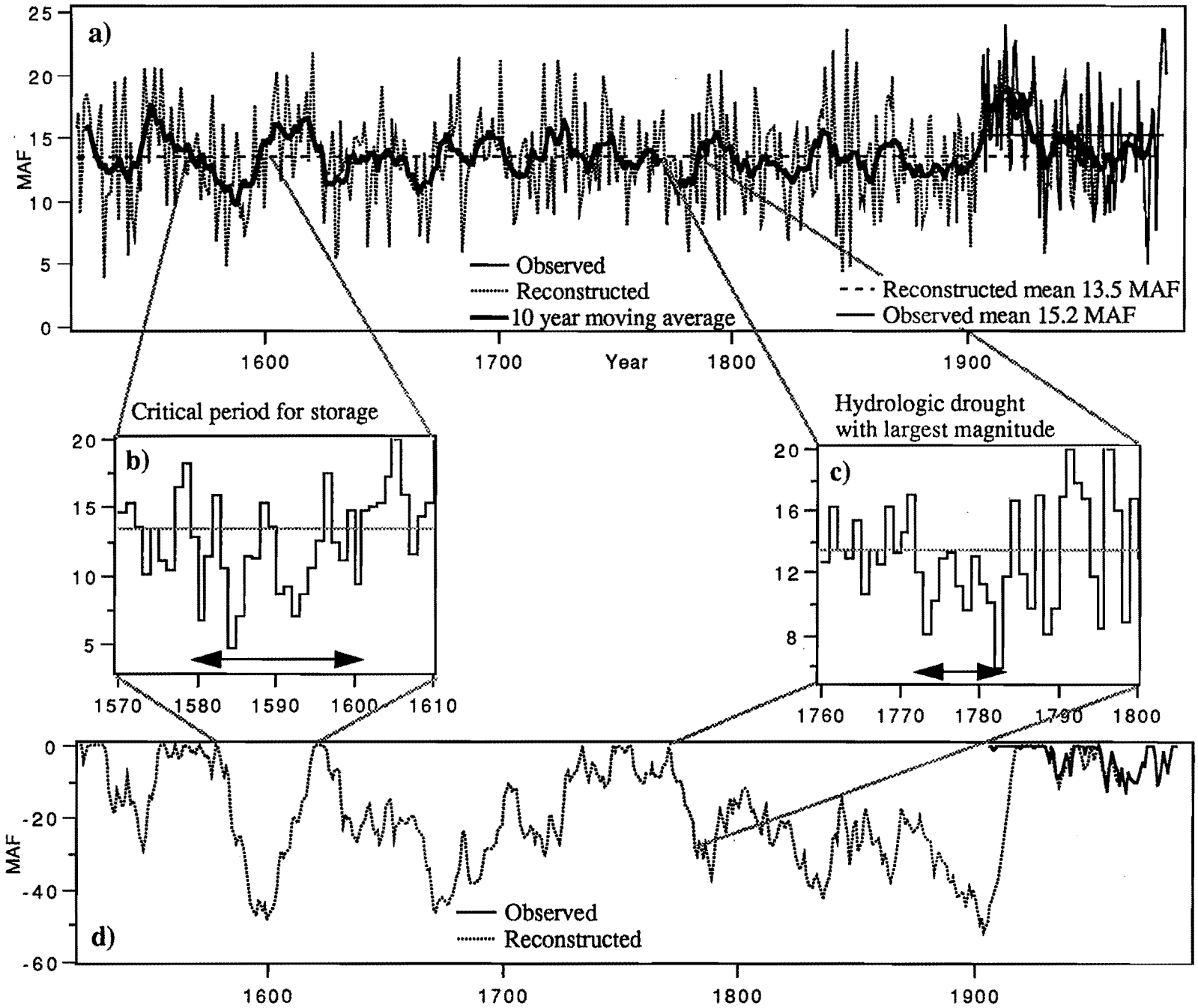
a)
MAF
Year
Observed
Reconstructed
10 year moving average
Reconstructed mean 13.5 MAF
Observed mean 15.2 MAF
Critical period for storage
b)
Hydrologic drought
with largest magnitude
c)
d)
Observed
Reconstructed

Figure 6.

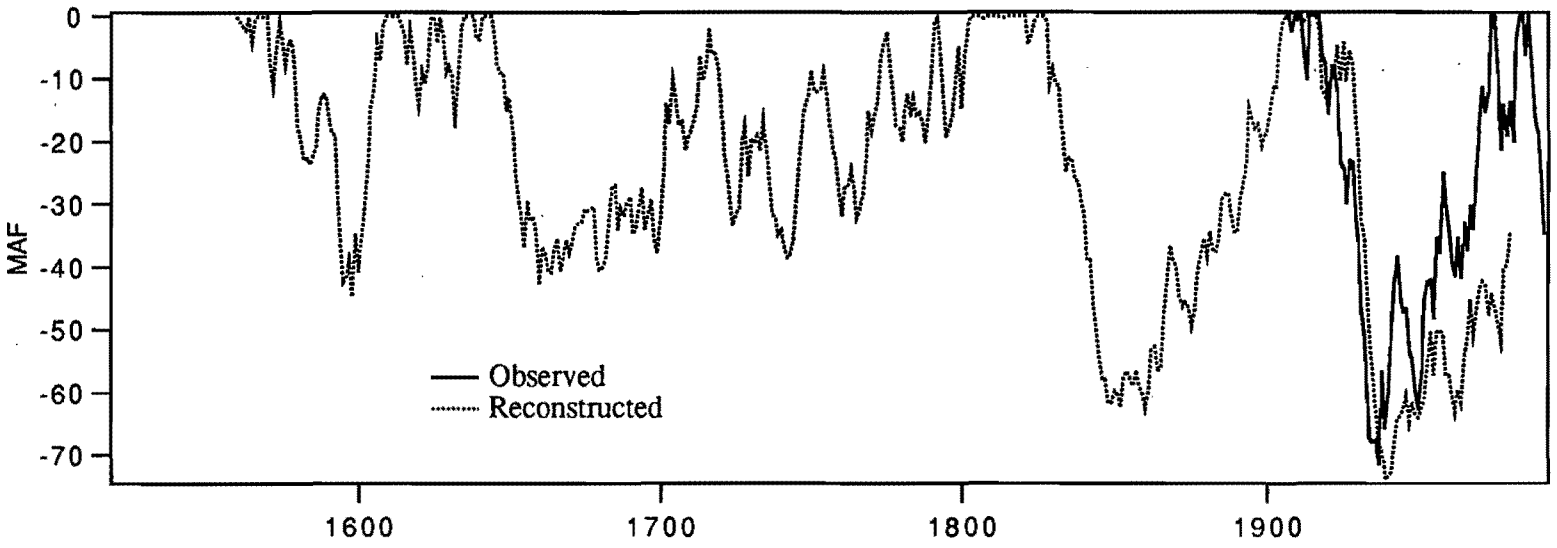
0
-10
-20
-30
-40
-50
-60
-70
MAF
Observed
Reconstructed
1600
1700
1800
1900

Figure 7.

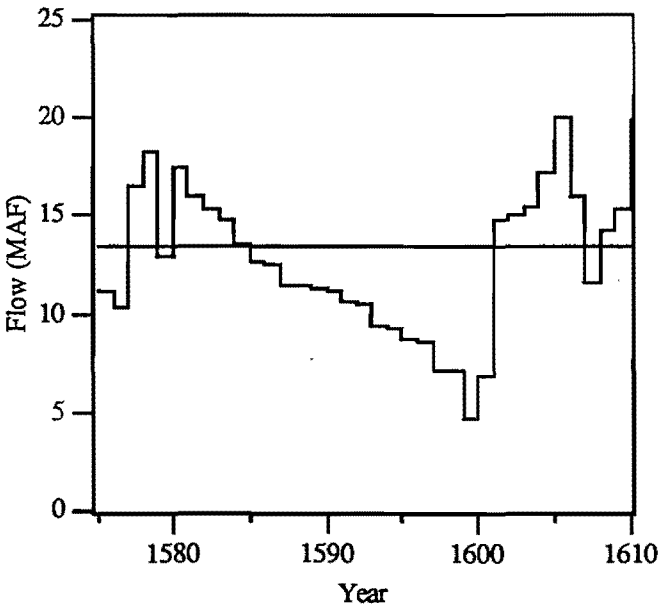

Figure 8. Colorado re-arranged severe drought

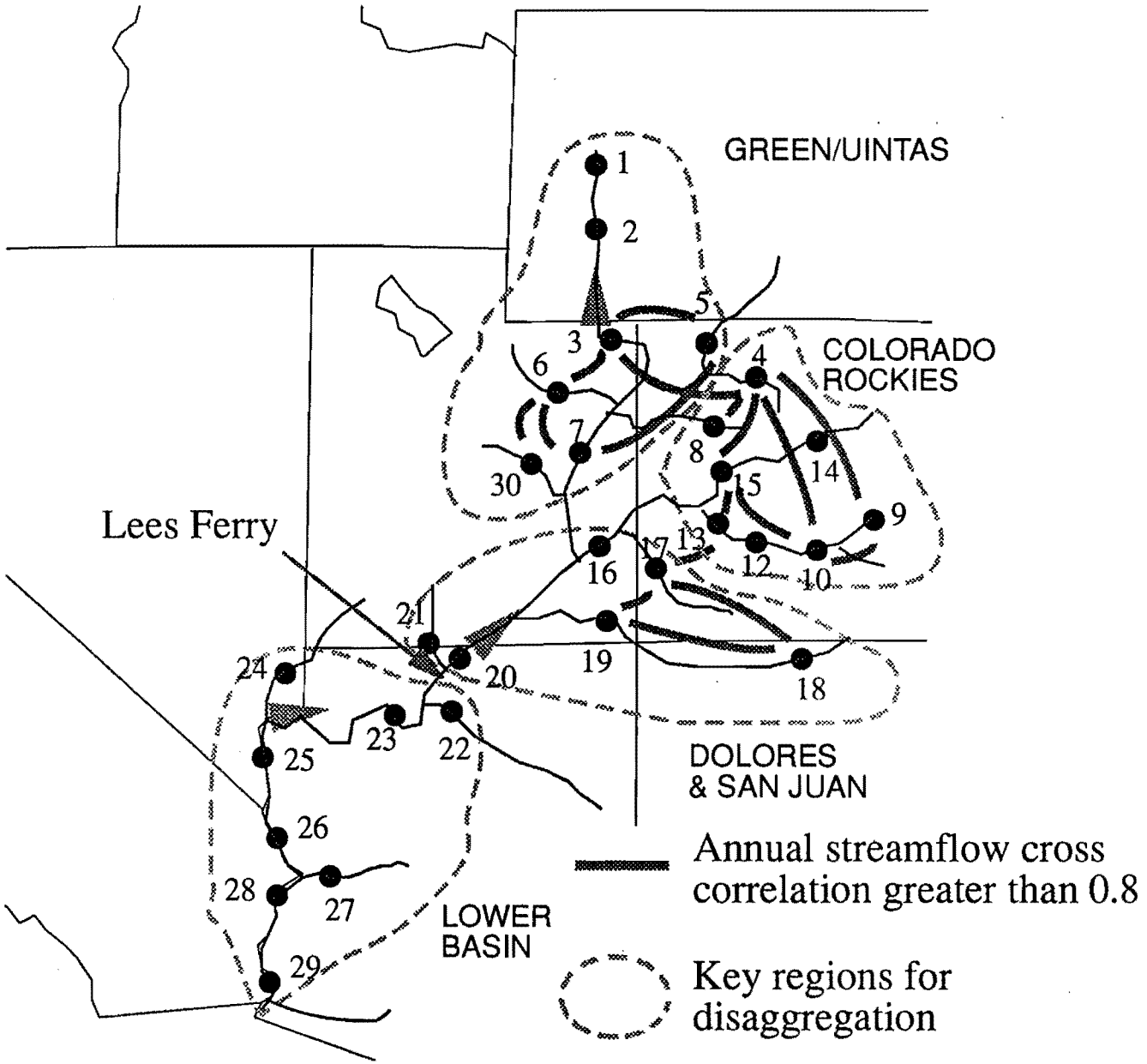
GREEN/UINTAS
COLORADO ROCKIES
Lees Ferry
DOLORES & SAN JUAN
LOWER BASIN
1
2
3
4
5
6
7
8
9
10
11
12
13
14
15
16
17
18
19
20
21
22
23
24
25
26
27
28
29
30
Annual streamflow cross correlation greater than 0.8
Key regions for disaggregation

Figure 9.

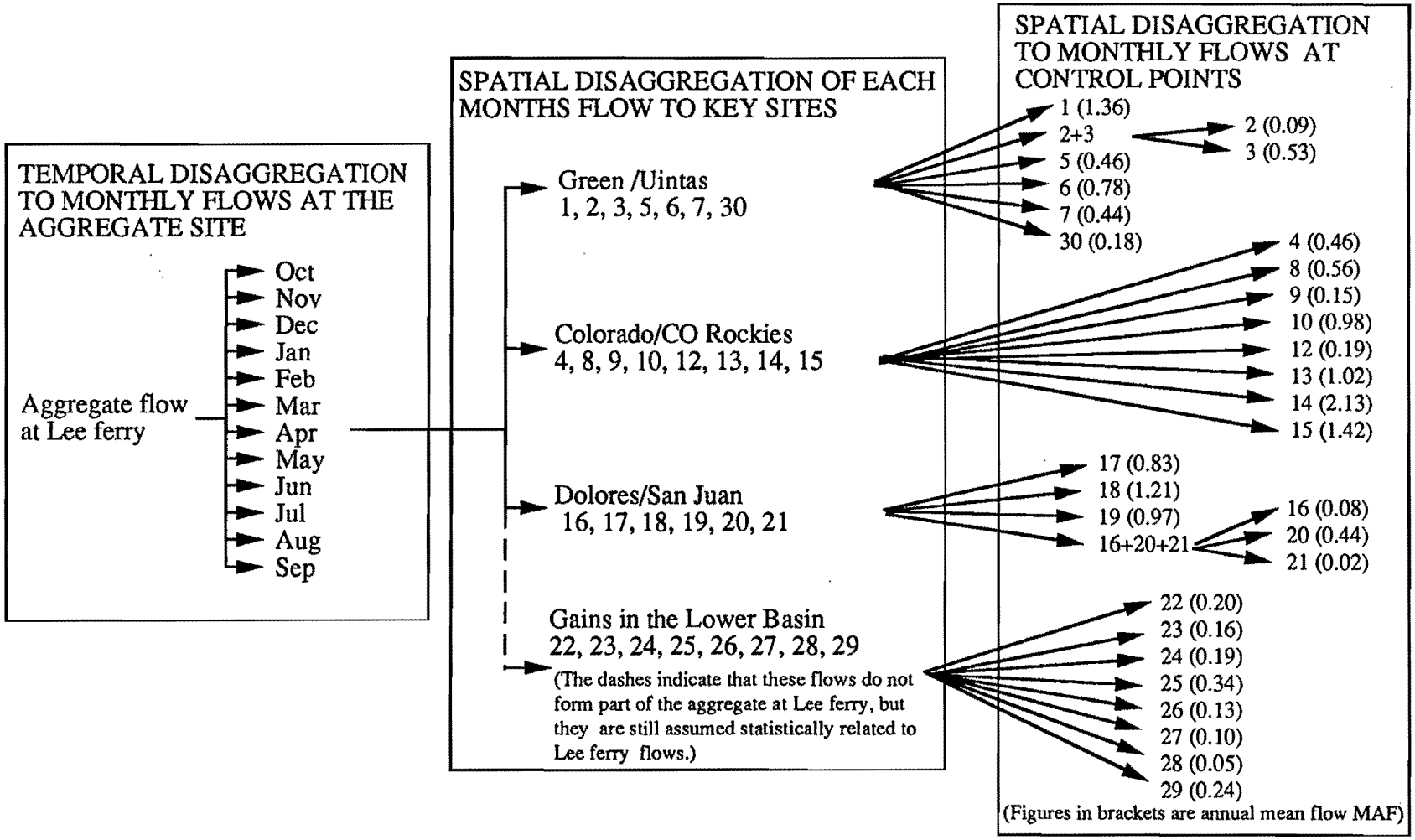

Structure of Disaggregation model for the Colorado System

FIGURE 10.

a. Green/Uintas October.

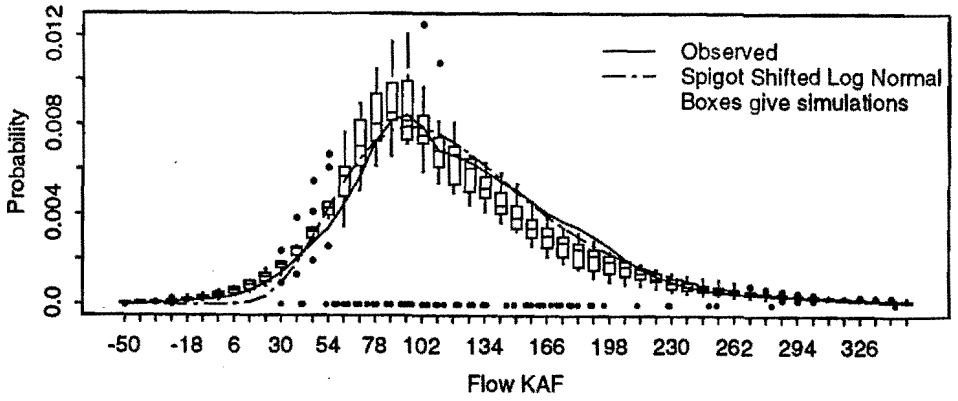

b. Green/Uintas January.

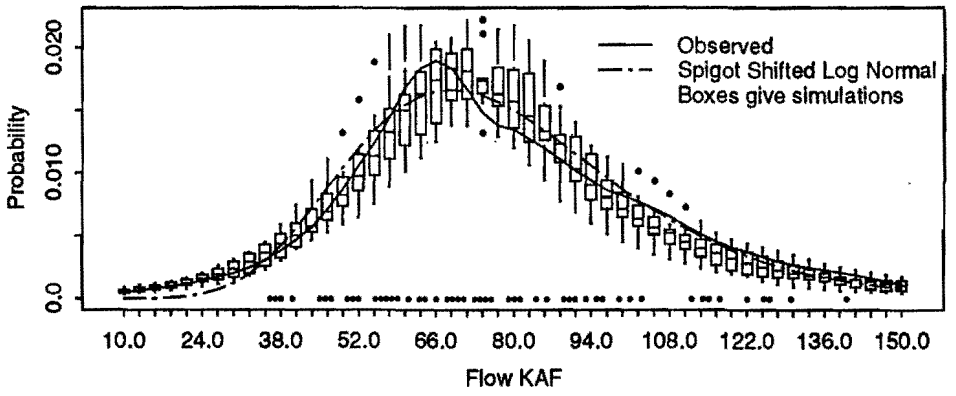

c. Source location 18 (San Juan) April.

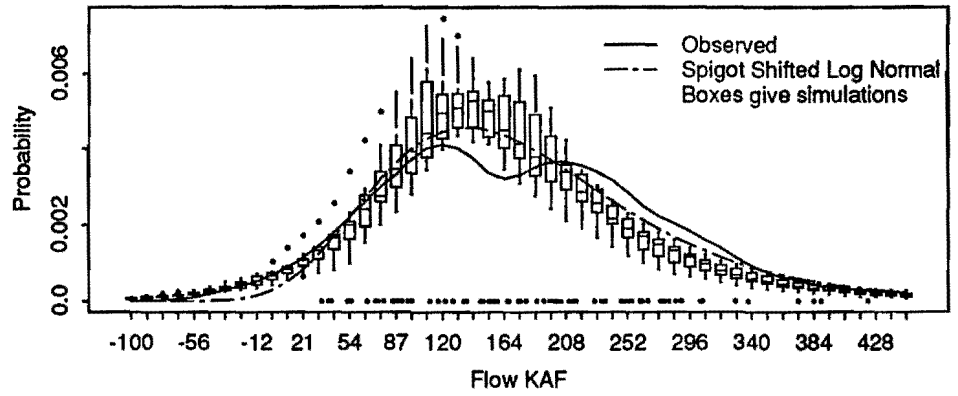

d. Source location 18 (San Juan) June.

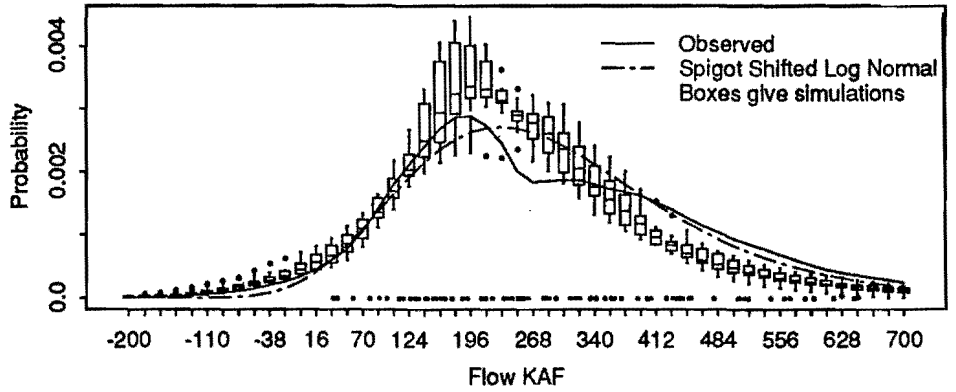

e. Source location 7 (Green gains) December.

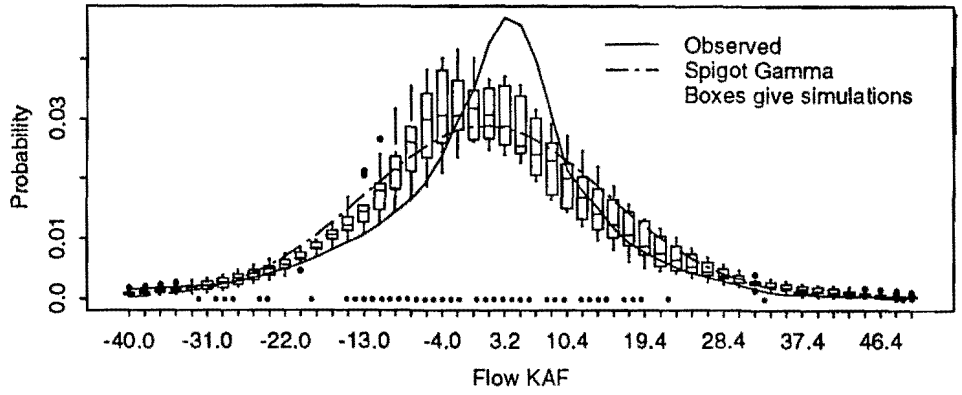

f. Source location 30 (San Rafael) February.

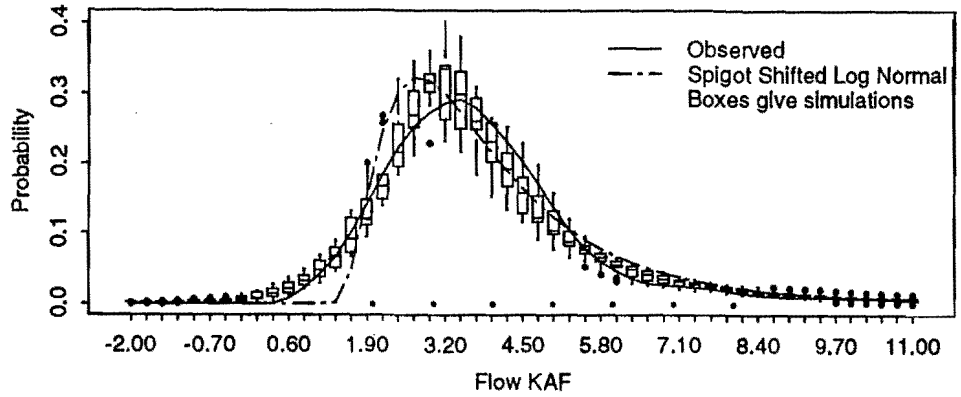

FIGURE 11

a. Source location 1, Mean flow.

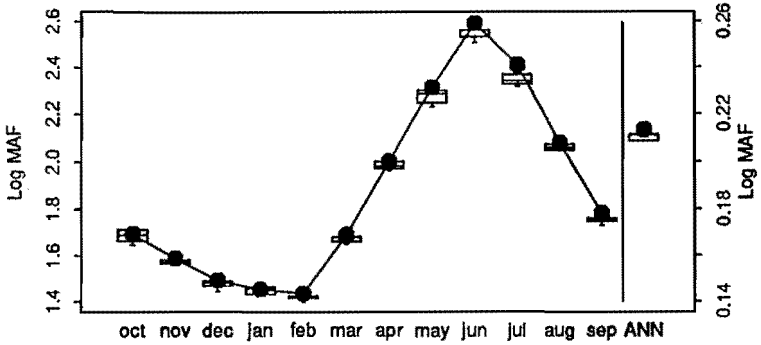

b. Source location 1, Standard deviation.

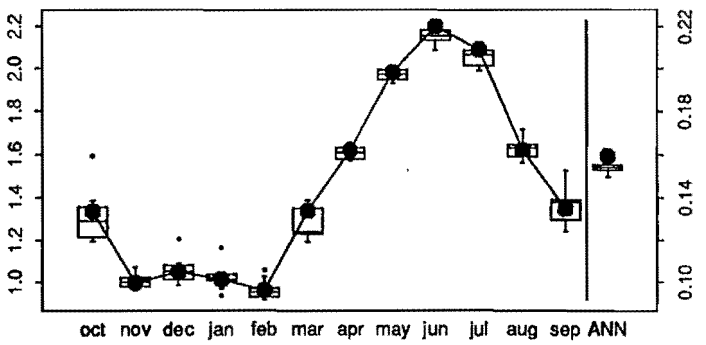

c. Source location 2, Mean flow.

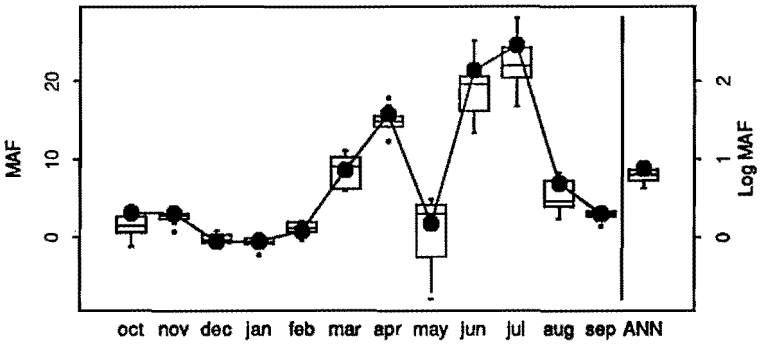

d. Source location 2, Standard deviation.

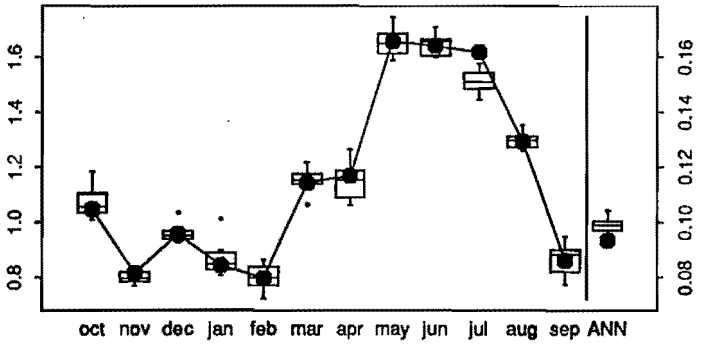

FIGURE 12

a. Source location 1, 10% quantile.

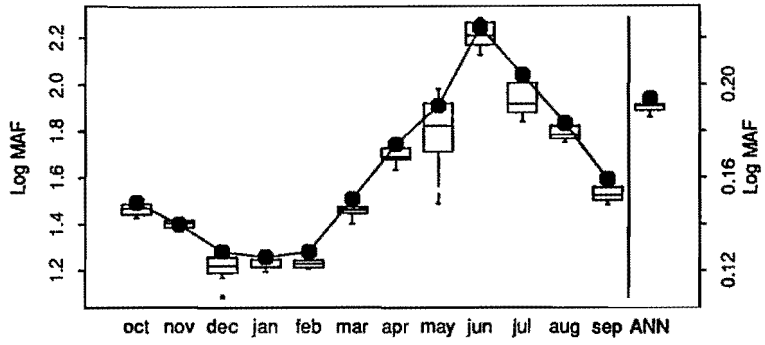

b. Source location 1, 90% quantile.

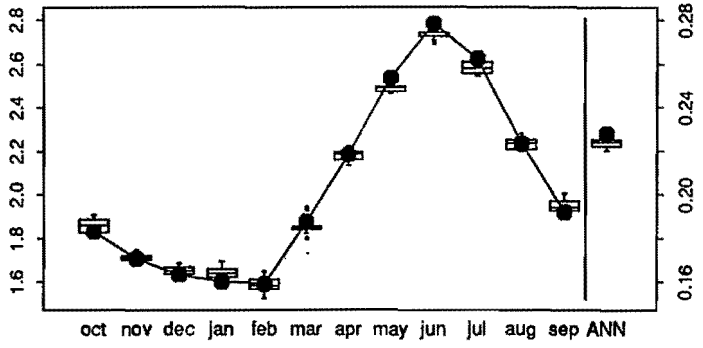

c. Source location 2, 10% quantile.

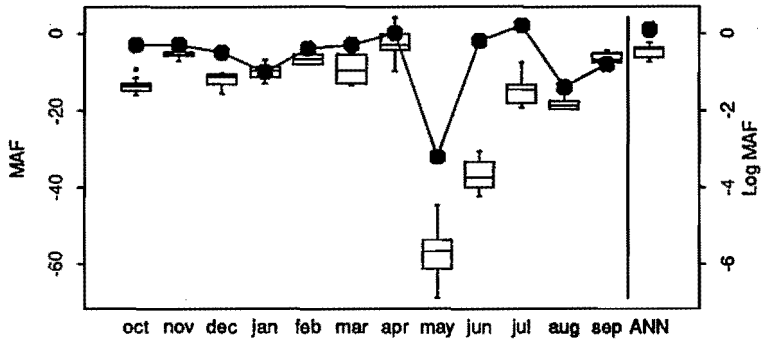

d. Source location 2, 90% quantile.

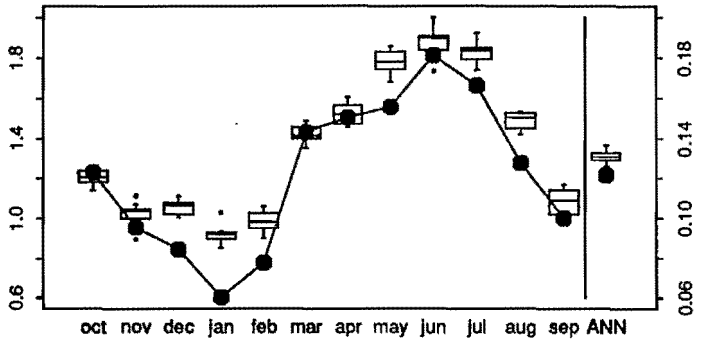

FIGURE 13

a. Green/Uintas Lag 1 autocorrelations

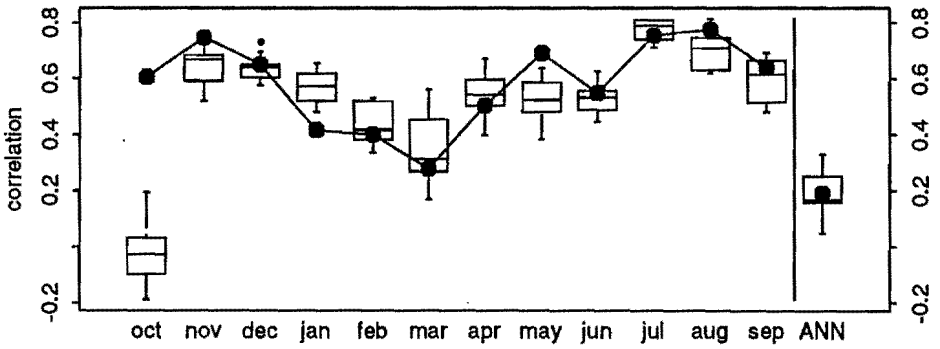

b. Green/Uintas Lag 2 autocorrelations

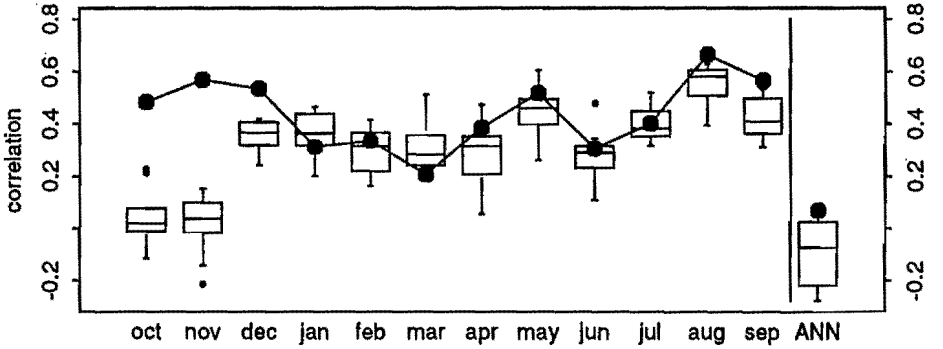

c. Green/Uintas Lag 3 autocorrelations

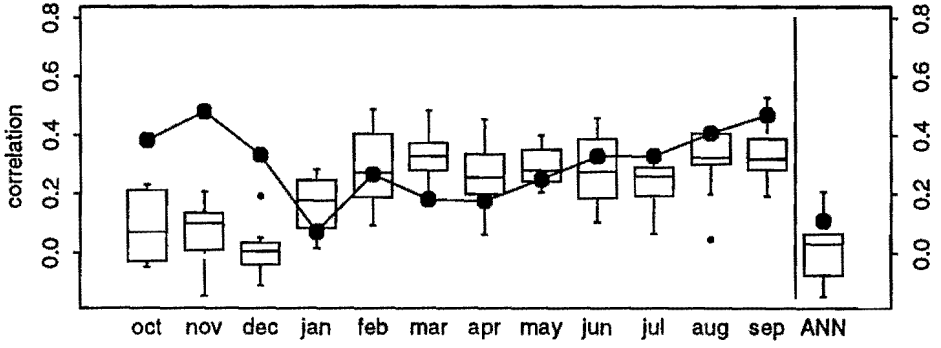

d. Green/Uintas Lag 4 autocorrelations

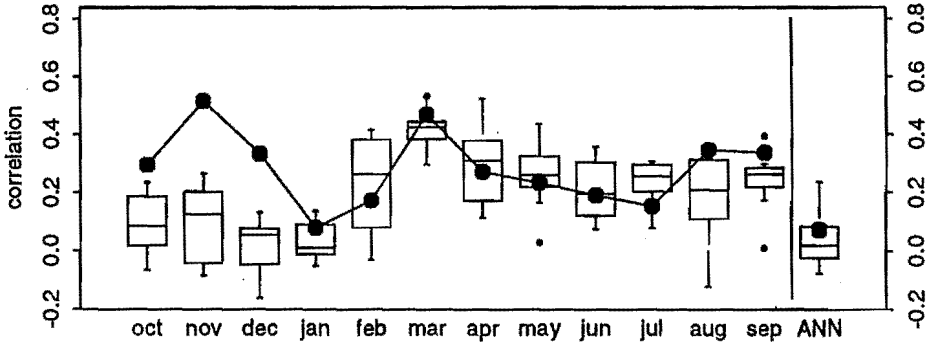

FIGURE 14

a. Source Locations 1 and 4 cross correlations.

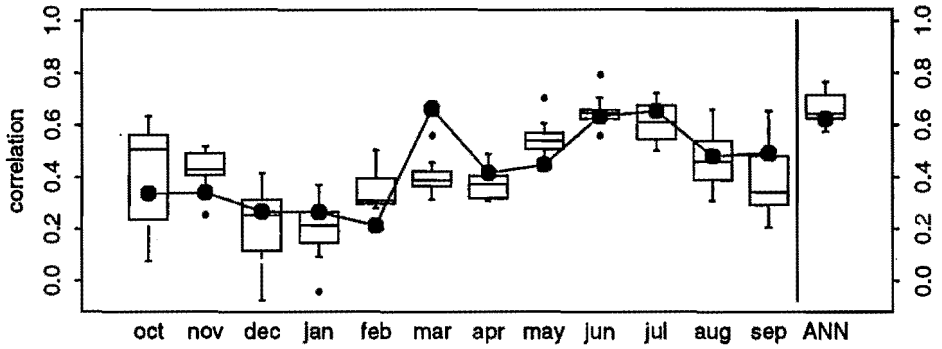

b. Source Locations 4 and 5 cross correlations.

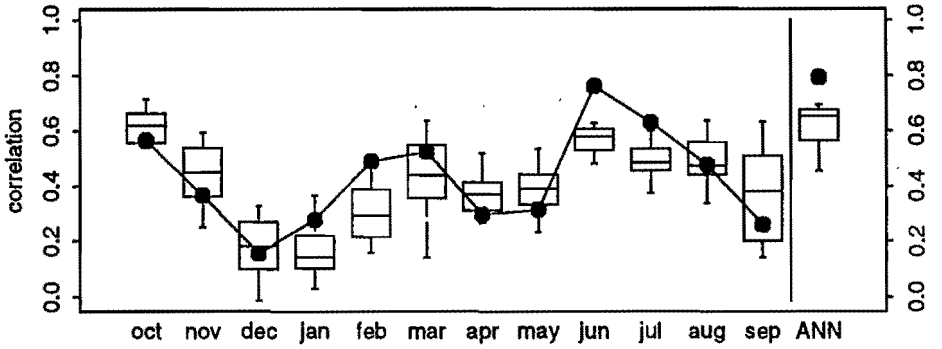

c. Source Locations 1 and 5 cross correlations.

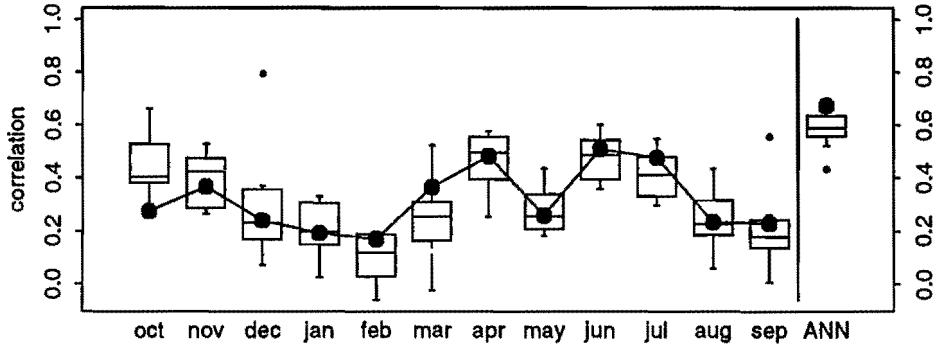

d. Source Locations 1 and Green/Uintas cross correlations.

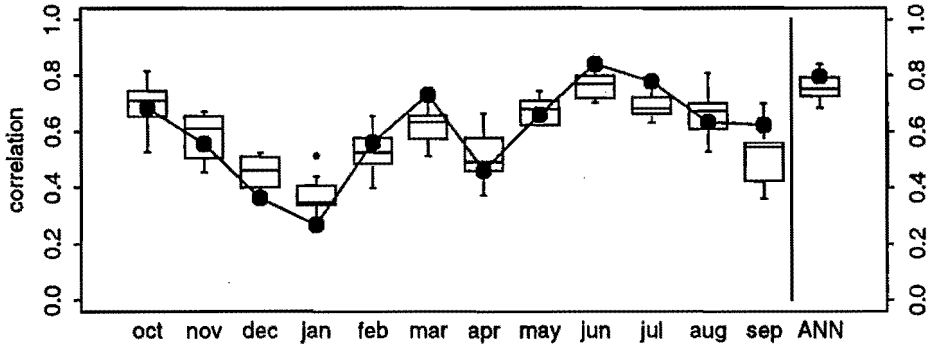

e. Green/Uintas and Colorado rockies cross correlations.

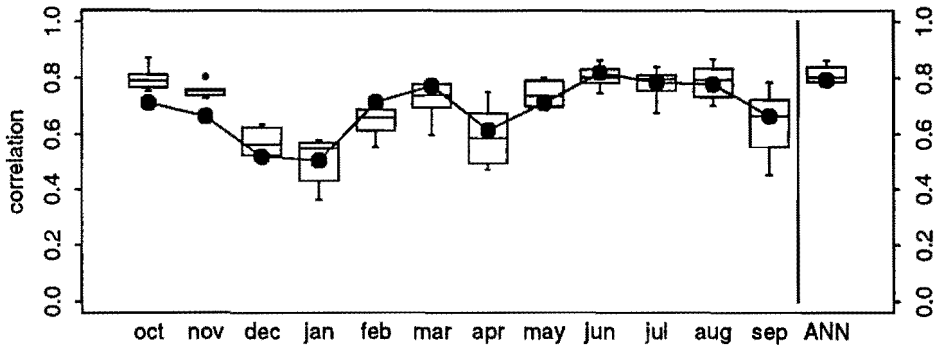

f. Green/Uintas and Lees Ferry cross correlations.

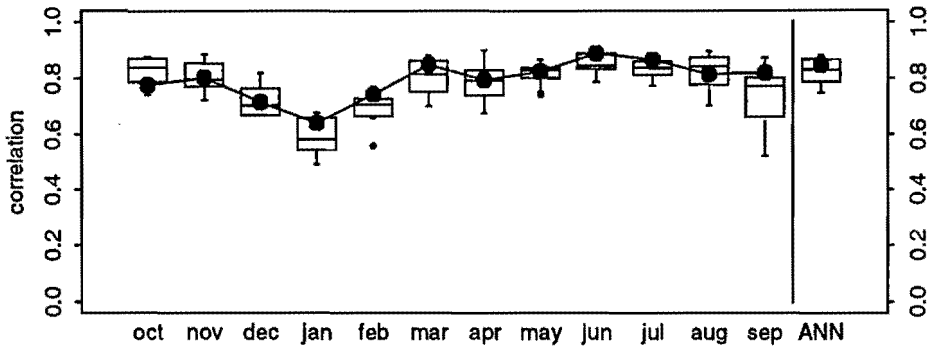

FIGURE 15

Gaussian Kernel

$$K(x) = \frac{1}{\sqrt{2\pi}} e^{-x^2/2}$$

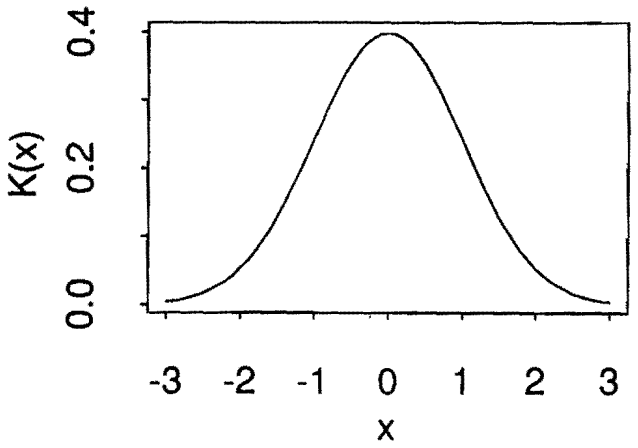

Epanechnikov Kernel

$$K(x) = \frac{3}{4\sqrt{5}} (1 - x^2/5) \qquad -\sqrt{5} < x < \sqrt{5}$$

$$= 0 \qquad |x| > \sqrt{5}$$

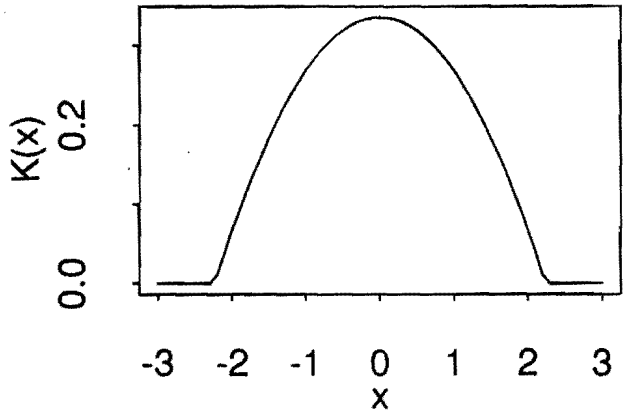

Figure A-1. Typical kernels for non parametric density estimation.

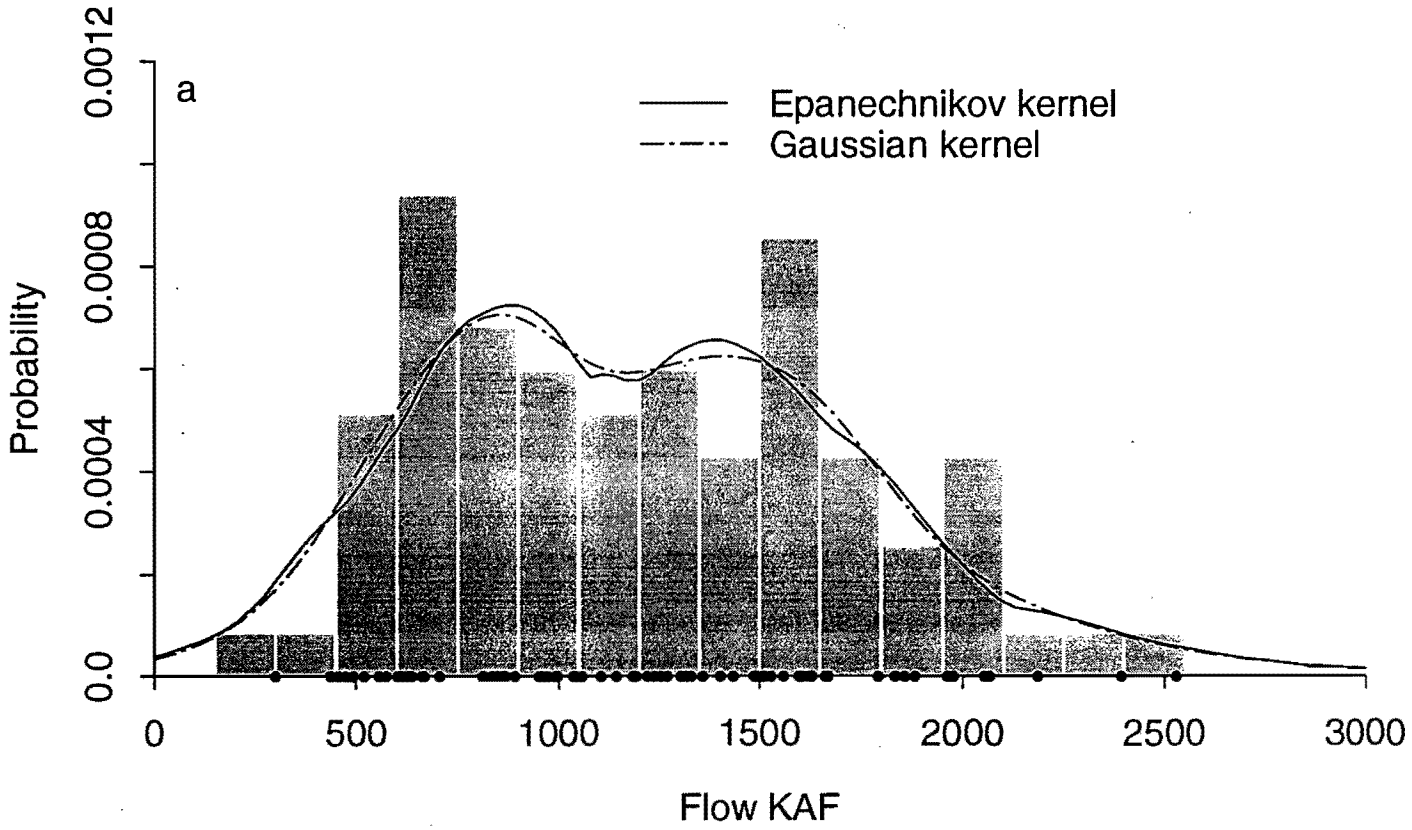
a
Epanechnikov kernel
Gaussian kernel
Probability
0.0
0.0004
0.0008
0.0012
0
500
1000
1500
2000
2500
3000
Flow KAF

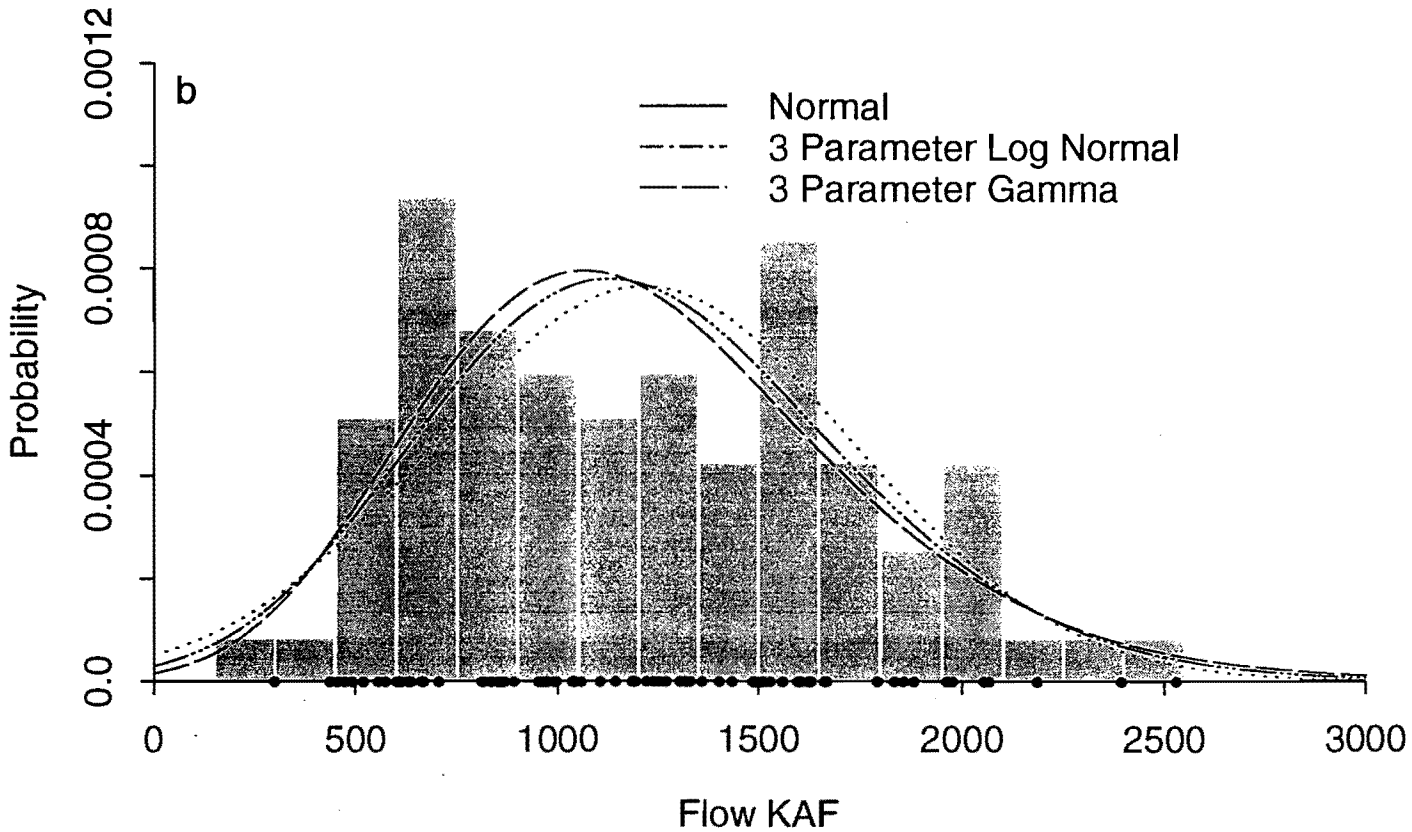
b
Normal
3 Parameter Log Normal
3 Parameter Gamma
Probability
0.0
0.0004
0.0008
0.0012
0
500
1000
1500
2000
2500
3000
Flow KAF

FIGURE A-2

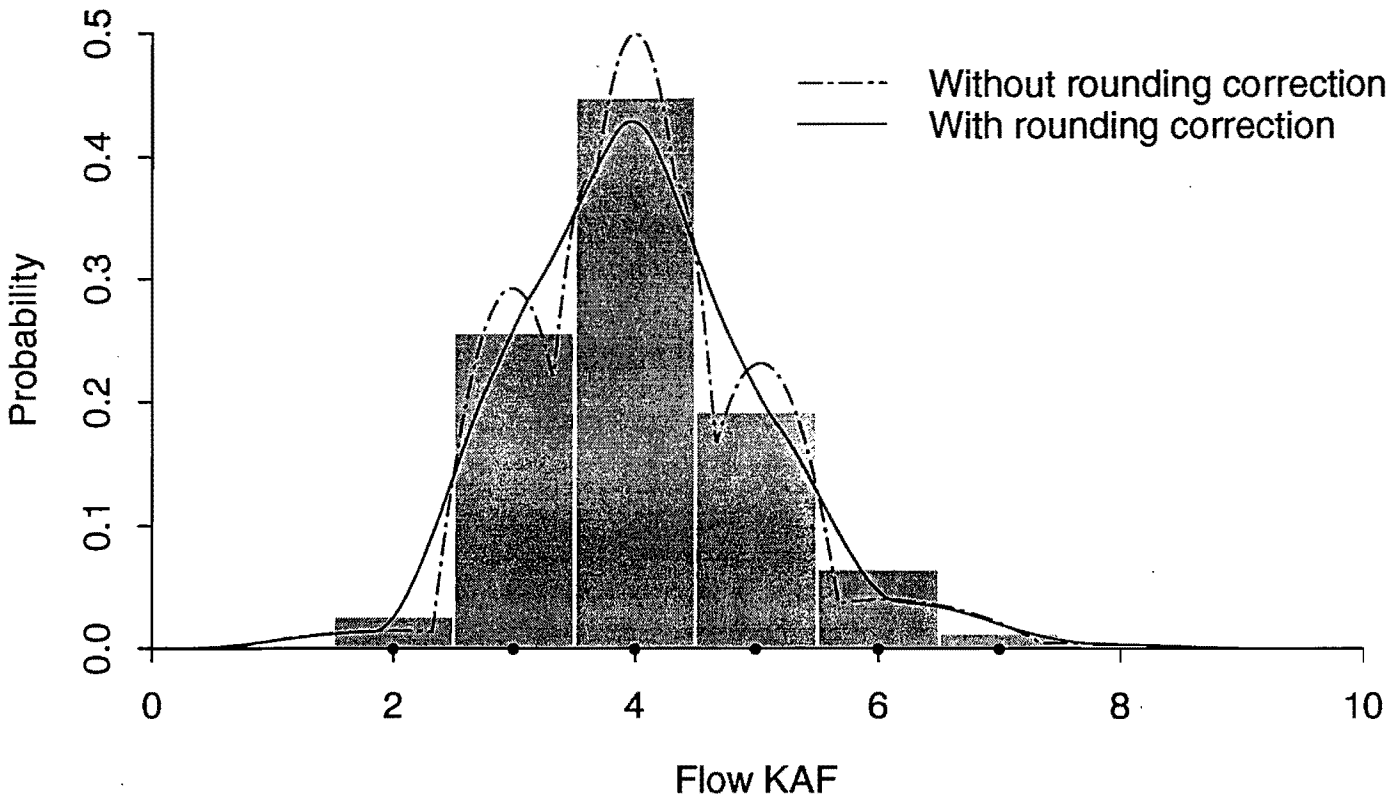
Without rounding correction
With rounding correction
Probability
0.0
0.1
0.2
0.3
0.4
0.5
0
2
4
6
8
10
Flow KAF

FIGURE A-3